Diapedesis-induced integrin signalling via LFA-1 facilitates tissue immunity by inducing intrinsic complement C3 expression in immune cells

Martin Kolev[1*], Erin E. West[1*], Natalia Kunz[1], Daniel Chauss[2], E. Ashley Moseman[3], Jubayer Rahman[3], Tilo Freiwald[2], Maria L. Balmer[4], Jonas Lötscher[4], Sarah Dimeloe[4,5], Elizabeth C. Rosser[6,7], Lucy R. Wedderburn[6,7,8], Katrin D. Mayer-Barber[9], Andrea Bohrer[9], Paul Lavender[10], Andrew Cope[10], Luopin Wang[11], Mariana J. Kaplan[12], Niki M. Moutsopoulos[13], Dorian McGavern[3], Steven M. Holland[14], Christoph Hess[4,15], Majid Kazemian[11**], Behdad Afzali[2**], Claudia Kemper[1,10,16,17**]

[1] *Complement and inflammation Research Section (CIRS), National Heart, Lung, and Blood Institute (NHLBI), National Institutes of Health (NIH), Bethesda, MD, 20892, USA;*
[2] *Immunoregulation Section, Kidney Diseases Branch, National Institute of Diabetes and Digestive and Kidney Diseases (NIDDK), NIH, Bethesda, MD, 20892, USA;*
[3] *Viral Immunology & Intravital Imaging Section, National Institute of Neurological Disorders and Stroke (NINDS), NIH, Bethesda, MD, 20892, USA;*
[4] *Department of Biomedicine, Immunobiology, University Hospital and University of Basel, Basel, 4031, Switzerland;*
[5] *Institute of Immunology and Immunotherapy, University of Birmingham, Birmingham, B15 2TT, UK;*
[6] *Infection, Immunity, Inflammation Programme, University College London (UCL) Great Ormond Street Institute of Child Health, London, WC1N 1EH, UK;*
[7] *Arthritis Research UK Centre for Adolescent Rheumatology at UCL, UCHL and GOSH, London, WC1N 1EH, UK;*
[8] *National Institute for Health Research (NIHR) Biomedical Research Centre at Great Ormond Street NHS Foundation Trust, London, WC1N 1EH, UK;*
[9] *Inflammation and Innate Immunity Unit, National Institute of Allergy and Infectious Diseases (NIAID), NIH, Bethesda, MD, 20892, USA:*
[10] *School of Immunology and Microbial Sciences, Faculty of Life Sciences and Medicine, King's College London, London, SE1 9RT, UK;*
[11] *Departments of Biochemistry and Computer Science, Purdue University, West Lafayette, IN, 47907, USA;*
[12] *Systemic Autoimmunity Branch, National Institute of Arthritis and Musculoskeletal and Skin Disease (NIAMS), NIH, Bethesda, MD, 20892, USA;*
[13] *Oral Immunity and Inflammation Unit, National Institute of Dental and Craniofacial Research (NIDCR), NIH, Bethesda, MD, 20892, USA;*
[14] *Laboratory of Clinical Immunology and Microbiology, National Institute of Allergy and Infectious Diseases (NIAID), NIH, Bethesda, MD, 20892, USA;*
[15] *Department of Medicine, University of Cambridge, Cambridge, CB2 0AW, UK;*
[16] *Institute for Systemic Inflammation Research, University of Lübeck, Lübeck, 23562, Germany*
[17] *Lead contact*

* These authors contributed equally

** Senior and corresponding authors

Contacts for correspondence: kazemian@purdue.edu; behdad.afzali@nih.gov; claudia.kemper@nih.gov

Summary

Intrinsic complement C3 activity is integral to human Th1 and cytotoxic T cell responses. Increased or decreased intracellular C3 results in autoimmunity and infections, respectively. The mechanisms regulating intracellular C3 expression remain undefined. We identified complement, including C3, as among the most significantly enriched biological pathway in tissue-occupying cells. We generated *C3*-reporter mice and confirmed that C3 expression was a defining feature of tissue-immune cells, including T cells and monocytes, occured during trans-endothelial diapedesis, and depended on integrin LFA-1 signals. Immune cells from patients with leukocyte adhesion deficiency (LAD)-1 had reduced *C3* transcripts and diminished effector activities, which could be rescued proportionally by intracellular C3 provision. Conversely, increased *C3* expression by T cells from arthritis patients correlated with disease severity. Our study defines integrins as key controllers of intracellular complement, demonstrates that perturbations in the LFA-1-C3-axis contribute to primary immunodeficiency and identifies intracellular C3 as biomarker of severity in autoimmunity.

Keywords:

Intracellular complement, complosome, T cells, LFA-1, ICAM-1, integrins, metabolism, Th1 cells, lymphocyte adhesion deficiency type 1, LAD-1, biomarker

Introduction

The complement system is an evolutionarily conserved immune sensor critical for protection against invading pathogens. Upon pathogen sensing, proteolytic activation of liver-derived and serum-circulating complement component C3 generates C3a and C3b and of C5 generates C5a and C5b. These activation fragments lead to opsonization and lytic killing of invading pathogens, recruitment and activation of innate immune cells and induction of inflammatory responses (Merle et al., 2015; Ricklin et al., 2010). Recent studies have found that the complement system has additional, non-canonical, functions that critically regulate human adaptive T cell responses and that are largely independent of serum-derived C3 and C5 (West et al., 2018). In fact, key to the control of human adaptive T cell responses is T cell-intrinsic, intracellular, expression of C3 and C5 and generation of activation fragments of these components intracellularly (Cardone et al., 2010; Liszewski et al., 2013). C3a and C3b are continuously generated intracellularly at low levels in resting T cells via cathepsin L-mediated cleavage of C3. The engagement of the lysosomal-expressed G-protein coupled C3a receptor (C3aR) via intracellularly generated C3a sustains tonic mammalian target of rapamycin complex 1 (mTORC1) activity and homeostatic survival of circulating T cells (Liszewski et al., 2013). T cell receptor (TCR) activation and CD28 co-stimulation increases cathepsin L-mediated activation of C3 and induces shuttling of C3 activation fragments to the cell surface. Here, they engage their respective receptors, C3aR (which binds C3a) and CD46 (which binds C3b), to induce interferon (IFN)-γ production and T helper type (Th) 1 differentiation (Liszewski et al., 2013). The same pathway functions in human $CD8^+$ cytotoxic T lymphocytes (CTLs) – C3 protein is processed intracellularly to activation fragments that engage the same receptors in an autocrine/paracrine manner – and drive optimal IFN-γ production and cytolytic activity (Arbore et al, 2018).

Mechanistically, CD46 engagement licenses appropriate T cell metabolism to induce Th1 differentiation and CTL activation. CD46-mediated signals permit nutrient influx via expression of the glucose transporter 1 (GLUT1) and the large neutral amino acid (AA) transporter (LAT) 1 during T cell activation (Hess and Kemper, 2016; Kolev et al., 2015). Autocrine CD46 activation simultaneously drives assembly of the AA-sensing mTORC1 complex to lysosomes. These processes together enable glycolytic and oxidative phosphorylation (OXPHOS) bursts required for IFN-γ production and Th1 specification (Figure

S1A) (Chang et al., 2013; Delgoffe et al., 2009; Hess and Kemper, 2016; Kolev et al., 2015). In CTLs, CD46 augments fatty acid synthase which is required for normal CTL effector function (Arbore et al., 2018). CD46 also operates upstream of intracellular C5 pools that generate C5a and engage the mitochondrial-expressed C5aR1 to trigger assembly of an intrinsic NLR family pyrin domain containing 3 (NLRP3) inflammasome in $CD4^+$ T cells, which in turn regulates the duration of Th1 responses in tissues (Arbore and Kemper, 2016; Arbore et al., 2016).

CD46-deficient patients suffer from recurrent infections and have severely reduced Th1 (but unaffected Th2) immunity (Le Friec et al., 2012). Similarly, $CD4^+$ T cells from C3-deficient patients display a specific defect in IFN-γ secretion early in life but have normal Th2 and Th17 cytokine production (Ghannam et al., 2014; Jiménez-Reinoso et al., 2018). Conversely, pathologically increased intracellular C3 activation in T cells contributes to the hyperactive Th1 responses observed in autoimmunity (Cardone et al., 2010; Ellinghaus et al., 2017; Liszewski et al., 2013) and can be normalized pharmacologically by inhibiting intracellular cathepsin L function (Liszewski et al., 2017; Liszewski et al., 2013).

Importantly, CD46 is not expressed on hematopoietic cells in rodents and a functional murine homologue mimicking the activities of human CD46 remains unelucidated (Tsujimura et al., 1998; West et al., 2018). Furthermore, the C3-activating enzyme in mouse T cells remains unidentified. Indeed, although mouse $CD4^+$ T cells contain intracellular processed C3a and express cathepsin L (Ctsl), this enzyme does not process murine intracellular C3 (Liszewski et al., 2013). Thus, homeostatic survival as well as the magnitude and duration of normal Th1 and CTL responses in humans is regulated via a species-specific intracellular complement system (the complosome), aberrant activity of which contributes to a range of human diseases. The ability to control key complosome components could, therefore, have great therapeutic impact.

The mechanisms that regulate *C3* (and *C5*) gene expression in T cells are currently undefined as TCR and/or CD28 engagement induce proteolytic activation of existing C3 pools but not *C3* gene transcription itself (Liszewski et al., 2013). Thus, the upstream signal(s) inducing the augmented intracellular expression of *C3* necessary for induction of normal T cell effector responses are currently unknown. We report here that we identified cell-intrinsic transcription of the complement system, including *C3*, as one of the most significantly

enriched biological pathway in tissue-occupying immune cell populations, including macrophages, $CD4^+$ and $CD8^+$ T cells. We further showed that engagement of the integrin lymphocyte function-associated antigen 1 (LFA-1, or CD11a/CD18) on immune cells by intercellular adhesion molecule 1 (ICAM-1) during endothelial transmigration and/or antigenic stimulation was key to the induction of cell-intrinsic *C3* gene expression. Accordingly, defective Th1, CTL and monocyte responses evident in patients with LFA-1 deficiency correlated with reduced intracellular stores of C3 and, as principally tested for their $CD4^+$ T cells, could be proportionally corrected through forced over-expression of C3 or C3a protein. Conversely, 'diapedesed' T cells isolated from the inflamed joints of patients with rheumatoid arthritis (RA) displayed augmented steady-state mRNAs encoding *C3* and *IFNG* when compared to their blood-circulating counterparts. *C3* transcript expression by these cells was associated with disease severity and acted as a biomarker distinguishing inflamed versus uninflamed RA.

Together, this study identified a functionally critical role for the integrin network as a key regulator of intracellular/autocrine complement and suggests that the complosome is an important feature of protective immunity in tissues. Furthermore, we provided mechanistic insights into a primary immunodeficiency disease resulting from LFA-1 deficiency and identified T cell *C3* production as a biomarker of the severity of autoimmunity.

Results

Complement *C3* gene transcription is a specific feature of immune cells in tissue

Human $CD4^+$ T cells require low-levels of intracellular C3a for homeostatic survival (Liszewski et al., 2013). However, successful Th1 induction needs a substantial rise in intracellular C3 protein above the 'maintenance level' to achieve the increased autocrine C3aR and CD46 engagement that drives metabolic reprogramming (Figure S1A) (Kolev et al., 2015; Liszewski et al., 2013). How this occurs is currently unknown. Because antigen presentation and T cell activation occurs in lymph nodes, we hypothesized that the process of diapedesis from the periphery into tissues may trigger intrinsic *C3* gene transcription and its related pathways in transmigrating T cells. To test this hypothesis, we first performed geneset enrichment analysis (GSEA) (Subramanian et al., 2005) on all (*n* = 2199) canonical pathways curated by the MSig database, comparing the transcriptomes of tissue (lung) and splenic (a proxy for blood) human $CD4^+$ T cells from the dataset of (Kumar et al., 2017) (GSE94964). 886 pathways were enriched in lung compared to splenic $CD4^+$ T cells (Table S1). Of these, the topmost significantly enriched was the complement pathway (Table S1, Figures 1A and S1B) and an additional 11 were integrin-related pathways (Table S1 and Figure 1A). To determine whether this observation was specific to $CD4^+$ T cells or true for other immune cells as well, we performed a similar analysis for $CD8^+$ T cells, comparing the transcriptomes of tissue (lung) versus splenic human $CD8^+$ T cells (GSE94964) and the transcriptomes of tissue macrophages versus blood monocytes (GSE117970). In $CD8^+$ T cells, the complement pathway was again the most highly enriched, out of the 523 enriched pathways in tissue-occupying cells, and ten pathways were again associated with integrins (Table S1, Figures 1B and S1C). For myeloid cells, we identified 129 enriched pathways in tissue macrophages, of which the complement pathway was in the top quartile (Table S1, Figures 1C and S1D). The *C3* gene was among the "leading edge" (core enriched transcripts) of the most highly enriched complement pathways in tissue $CD4^+$ T cells, $CD8^+$ T cells and also macrophages (Figures S1B-D). Indeed, *C3* mRNA was substantially induced in all three cell types within tissues (Figures 1D-F).

To monitor *in vivo* induction of *C3* gene transcription, we inserted an IRES-Td tomato cassette after the stop signal into the endogenous murine *C3* locus to generate a *C3*-Td

tomato (C3-TdT) mouse acting as a reporter of *C3* gene transcription (Figures S1E-H). Live intravital imaging of an MRSA ear infection model in these mice confirmed that tissue-infiltrating immune cells were Td tomato-positive and, therefore, transcribing *C3* (Figures 1G-H and Movie S1). We corroborated by flow cytometry that $CD4^+$ T cells and $CD8^+$ T cells transcribed the *C3* gene at insignificant or basal levels in blood, spleen or draining lymph nodes but that active *C3* gene transcription became prevalent in cells that had migrated into the tissue (Figure 1I). Likewise, we verified active transcription of *C3* by tissue macrophages (Figure 1J). Collectively, these data indicated that *C3* gene transcription was largely a property of tissue-localized, rather than circulating, immune cells, suggesting that transmigration from blood to tissue may be a pre-requisite.

ICAM-1 is a driver of *C3* gene transcription in immune cells

Intracellular C3 activity is a critically integral component of human Th1 induction (Kolev et al., 2013; Liszewski et al., 2013). Utilizing an *in vitro* activation assay under serum-free conditions – to exclude C3 protein uptake – we screened a range of key adhesion molecules involved in the process of cell diapedesis (Figures 2A and S2A) (Muller, 2011) for their ability to stimulate IFN-γ secretion in activated naive or memory human $CD4^+$ T cells (as a surrogate read-out for *C3* gene induction). The integrins ICAM-1 and VCAM-1 were the only adhesion molecules that significantly increased IFN-γ secretion in activated T cells, with ICAM-1 being more potent and capable of enhancing production of IFN-γ in CD3-activated naive T cells (Figure S2A). To determine whether ICAM-1 engagement induced *C3* gene transcription, we activated naive $CD4^+$ T cells from the *C3*-TdT reporter mouse *in vitro* in the presence of ICAM-1 and observed a dose-dependent increase in *C3* reporter activity with increasing concentrations of ICAM-1 (Figure 2B). In both naive and memory human $CD4^+$ T cells, ICAM-1 in the absence of concurrent T cell receptor (TCR) engagement caused transcription of *C3* mRNA within 12h and detectable transcript and protein for approximately 24-36h (Figure 2C) but without IFN-γ production (Figure S2A). Co-engagement of the TCR, with and without other co-stimulatory signals, together with ICAM-1 prolonged *C3* mRNA and protein loading within T cells (Figures 2D-E and S2B-C) and induced IFN-γ (Figure S2A). This suggested that ICAM-1 engagement induced C3 accumulation but was insufficient to initiate Th1 differentiation without appropriately timed TCR signals for C3 processing (Liszewski et al., 2013). Further

support for LFA-1 as an upstream component of the C3–Th1 axis were observations that LFA-1 engagement only slightly increased the very low amounts of IL-4 and IL-17 protein produced by memory T cells under non-skewing activation conditions (Figure S1D). In fact, ICAM-1 suppressed both Th2 and Th17 cytokines during Th2 and Th17 differentiation from naive cells (Figure S2E). ICAM-1 also stimulated transcription of *C3* in both human $CD8^+$ T cells and monocytes, which was accompanied by enhanced effector activity (Figures S2F-I). Notably, *C3* transcription was accompanied in $CD8^+$ T cells by augmented production of cytokines (IFN-γ) and cytolytic factors (granzyme B and CD107 expression) and in monocytes by production of IL-1β (but not IL-6 or TNF) (Figures S2F-I).

In summary, these data showed that ICAM-1 was a key inducer of *C3* transcription in $CD4^+$ T cells, $CD8^+$ T cells and monocytes and established a temporal association between ICAM-1 engagement, C3 transcription and effector function in all three cell types.

ICAM-1–LFA-1 interaction during diapedesis is required for *C3* gene transcription

Because human $CD4^+$ T cells and Th1 induction are critically dependent on the function of intracellular C3, we focussed subsequent mechanistic studies around this T cell sub-population. Leukocyte function antigen (LFA)-1 is the major cognate ligand for ICAM-1 on T cells. LFA-1 is a heterodimer composed of two members of the integrin family, α_L (CD11a) and β2 (CD18) (Walling and Kim, 2018). To investigate whether ICAM-1 was intrinsically dependent on interaction with LFA-1, we measured *C3* mRNA and IFN-γ production in dense $CD4^+$ T cell cultures in the presence and absence of an inhibitory anti-LFA-1 antibody. As TCR engagement induces both LFA-1 activation and ICAM-1 expression on T cells (Walling and Kim, 2018), homotypic T cell-T cell-interactions in these cultures foster *in trans* LFA-1–ICAM-1 interactions and drive paracrine IL-2 signaling, which supports IFN-γ production (Doh and Krummel, 2010; Sabatos et al., 2008). We observed that CD18 blockade significantly reduced *C3* gene transcription and IFN-γ secretion under all co-activation conditions assessed (Figure S3A-B). Because LFA-1 shares the CD18 chain with the integrin macrophage-1 antigen (MAC-1, or CD11b/CD18), which is induced on activated human T cells (Wagner et al., 2001), we next tested MAC-1 ligation using its ligand iC3b, which is also generated by activated T cells in an autocrine fashion. iC3b was unable to trigger IFN-γ

production (Figure S3C), suggesting that the CD11a/CD18 heterodimer (LFA-1) was the functional ligand for ICAM-1-induced C3 loading and Th1 induction.

We next probed if the LFA-1 signaling mediates *C3* gene transcription in a more physiological setting during the actual process of T cell transmigration. We employed an *in vitro* trans-well system utilizing human umbilical vein endothelial cells (HUVEC) in which ICAM-1 expression could be controlled through IL-1β treatment (Hosokawa et al., 2006) (Figures 3A and S3D). The observed transmigration of both naive and memory T cells through the HUVEC monolayer was dependent on the LFA-1–ICAM-1 interaction, since addition of the developmental endothelial locus 1 (DEL-1) protein, which is an endogenous and specific inhibitor of the ICAM-1–LFA-1 interaction, abrogated T cell transmigration induced after IL-1β treatment of HUVECs (Choi et al., 2008) (Figure 3B). Moreover, LFA-1–ICAM-1-mediated transmigration of both naive and memory $CD4^+$ T cells induced both *C3* and *IFNG* transcription and C3 protein generation (Figures 3C-D and S3E). This effect was specific to Th1 induction, as neither *IL4* nor *IL17A* gene transcription were significantly induced (Figure S3F-G).

Since chemokines are also important for diapedesis, we tested the ability of a range of chemokines to induce IFN-γ and *C3* in the context of $CD4^+$ T cell activation. Only CXCL10 and CCL20 increased IFN-γ production and *C3* gene transcription (Figure S3H-J). Both CXCL10 and CCL20 activate conformational changes in LFA-1 that permit high-affinity interactions with ICAM-1 (Alcaide et al., 2012; Atarashi et al., 2005). Consistent with this, we found that blocking CD18 abolished the ability of CXCL10 and CCL20 to induce both IFN-γ and *C3* transcription (Figures S3I-J), indicating that both chemokines are dependent on ICAM-1 for regulating the *C3* gene.

Together, these data demonstrated that cognate LFA-1–ICAM-1 interactions during diapedesis induced transcription of *C3*.

ICAM-1 drives C3-dependent metabolic reprogramming during $CD4^+$ T cell activation

Processing of intracellular C3 generates both C3a and C3b and is enzymatically dependent on cathepsin L (CTSL) (Liszewski et al., 2013). To determine whether ICAM-1-ligation in the context of TCR stimulation is sufficient to trigger C3 protein processing and Th1 specification, we first cultured $CD4^+$ T cells in the presence and absence of a cell-permeable

CTSL inhibitor (CTSLi), which prevents intracellular C3 processing (Liszewski et al., 2013). ICAM-1 supported intracellular processing of C3 to C3a and stimulated IFN-γ production, both of which were abrogated by CTSLi, without reducing cell viability (Figures 4A and S4A-B). To corroborate these findings in cells with intrinsic C3 deficiency, we bred the C3 reporter mouse, which is floxed at the *C3* allele (Figure S1E), to a Cre-Deleter line of the same background and generated $C3^{-/-}$ mice. $C3^{-/-}$ $CD4^+$ T cells mice also showed impaired IFN-γ production (Figure S4C) and did not upregulate IFN-γ in response to ICAM-1, in contrast to cells from C3 wild-type animals (Figure S4D). In a transfer colitis experiment, recipients of $C3^{-/-}$ naive $CD4^+$ T cells had smaller spleens (Figure S4E) and a lower proportion of recovered $CD4^+$ T cells from the tissues of these mice expressed IFN-γ (Figure S4F). We also saw fewer IL-17A-expressing cells in recipients of $C3^{-/-}$ T cells (Figure S4G), indicating perhaps that the immunological effects of C3 deletion in murine T cells extends beyond simply Th1 differentiation.

Autocrine engagement of CD46 by T cell-derived C3b triggers glucose and AA influx and mTOR activation, which stimulate glycolytic and OXPHOS bursts essential for the metabolic demands connected with IFN-γ secretion and Th1 function (Figure S1A) (Chang et al., 2013; Kolev et al., 2015). ICAM-1-engagement during TCR activation resulted in similar metabolic changes in $CD4^+$ T cells, notably mTOR activation (measured by phosphorylation of the mTOR down-stream target S6 kinase) in activated bulk and sorted naive and memory T cells (Figures 4B and S4H). ICAM-1 also prompted significantly increased basal glycolysis and mitochondrial respiration, higher glycolytic capacity and maximal respiration as well as glycolytic reserve and spare respiratory capacity (Figures 4C and S4I-J) following TCR activation – particularly in naive and bulk T cells. All of these metabolic effects were reversible with CTSL inhibition (Figures 4C and S4I-J). Taken together, these data demonstrated that ICAM-1-dependent signalling was upstream of both *C3* gene transcription and CTSL-dependent intracellular C3 processing. These findings were corroborated in the context of intrinsic C3 deficiency, as $CD4^+$ T cells from the $C3^{-/-}$ mice also showed a clear defect in both glycolysis and oxidative phosphorylation (Figures S4K-N).

LFA-1 induces *C3* gene expression in $CD4^+$ T cells via AP-1

LFA-1 is part of the peripheral supramolecular activation cluster (pSMAC), formed on T cells after TCR engagement with antigen presenting cells (APC), and facilitates T cell activation (Dustin, 2008; Mempel et al., 2004; Rudolph et al., 2006). LFA-1-signaling synergizes and enhances TCR-triggered downstream pathways in an AP-1 and nuclear factor of activated T-cells (NFAT)-dependent manner (Bianchi et al., 2000; Kinoshita et al., 2012; Perez et al., 2003). Luciferase reporter assays have shown that the fish *C3* gene promotor has binding sites for the AP-1 family c-Fos–c-Jun heterodimer that can mediate AP-1-driven *C3* gene transcription *in vitro* (Chen et al., 2018). c-FOS ChIP-seq in human MCF10A cells confirmed binding of AP-1 family transcription factors within the *C3* promoter (Figure S5A) and motif analysis of the human *C3* promoter revealed the presence of DNA motifs for AP-1 binding (Figure S5B). Moreover, we found that LFA-1 ligation with ICAM-1 substantially enhanced abundance of *FOS* transcript and c-FOS protein in $CD4^+$ T cells stimulated with anti-CD3 (Figures S5C-D). We therefore assessed whether LFA-1-mediated *C3* gene transcription in human $CD4^+$ T cells was AP-1 dependent.

The addition of an AP-1 inhibitor into cultures during T cell stimulation at a concentration that left cell viability and proliferation of naive and memory T cells unaltered (Figure S5E) indeed abrogated LFA-1-induced *C3* gene expression (Figures 5A to D). This was not due to a general reduction in T cell fitness as expression of an unrelated control protein, CCR7, was not reduced, but in fact augmented, by AP-1 inhibition (Figure S5F). Thus, LFA-1 transduced an AP-1 signal that mediated transcription of the *C3* gene in human T cells.

LFA-1 deficiency diminishes *C3* expression and immune cell effector activity

To test the *in vivo* role of diapedesis in the induction of *C3* gene transcription in the context of disease, we isolated 'transmigrated' synovial $CD4^+$ T cells from the joints of patients suffering from idiopathic juvenile arthritis (Table S2) and adults with rheumatoid arthritis, together with paired blood-circulating T cells. At steady state, synovial T cells displayed augmented expression of *C3* and *IFNG* mRNA when compared to blood-circulating T cells (Figure 6A) and secreted significantly more IFN-γ upon *in vitro* re-stimulation (Figures S6A). Synovial T cells were refractory to ICAM-1 stimulation *in vitro*, whilst paired blood-derived T cells increased IFN-γ production 'normally' upon ICAM-1 exposure (Figure 6B). These data suggested that trans-migrating T cells *in vivo* acquired an active C3-Th1 signature similar to

that induced *in vitro* by TCR and LFA-1 engagement. To determine the *in vivo* relevance of *C3* gene transcription, we also examined RNA-sequencing data from synovial T cells of patients with rheumatoid arthritis from an independent dataset that included disease severity scoring (Immport SDY998) (Zhang et al., 2019). T cells of patients with inflamed RA expressed significantly more *C3* than those of patients with uninflamed RA (Figure 6C). Notably, *C3* mRNA expression by T cells distinguished inflamed RA from uninflamed RA (ROC AUC 0.70; $p<0.05$) and performed better as a biomarker of disease severity than *IFNG* mRNA (Figure 6D).

To further substantiate the requirement for integrin-dependent signaling in the induction of *C3* transcription and Th1 differentiation, we sourced blood from patients with leukocyte adhesion deficiency type-1 (LAD-1). LAD-1 is a rare autosomal recessive primary immune deficiency disease characterized by recurrent bacterial, viral and fungal infections. Patients have mutations in the *ITGB2* gene which encodes the CD18 integrin chain causing deficiency in all β2 integrins (Novoa et al., 2018). The recurrent infections in these patients are a consequence of absent/reduced LFA-1 expression and the inability of immune cells to migrate into sites of infection (Wolach et al., 2018). These patients also have exaggerated inflammatory responses in barrier tissues and a documented bias towards Th17 in mucosal inflammatory lesion, with the exact molecular pathways underlying this disease phenotype currently undefined (Moutsopoulos et al., 2017). We assessed $CD4^+$ T cells isolated from three patients, two of whom donated blood three times, with clinical manifestations ranging from mild to severe (Table S3), in comparison with T cells isolated from sex- and age-matched healthy donors. The proportion of circulating naive and memory T cells in these patients were within normal range (although with a trend towards an increased memory T cell pool), as was viability of resting and activated T cells (Figures S6B-C). Patients' T cells expressed normal protein amounts of CD46 (and TCR and CD28, not shown) and down-regulated CD46 expression upon CD46 stimulation in a similar manner to healthy donors (Yamamoto et al., 2013) (Figure S6D).

Compared to healthy controls, patients with LAD-1 had lower amounts of mRNA encoding *C3* (and intracellular C3a generation) both directly *ex vivo* and under all activation conditions tested, together with much lower production of IFN-γ (Figures 6E and S6E). IL-4 secretion was unaltered, and IL-17 output was increased in two patients (Figure S6F).

Importantly, patients and healthy donors demonstrated a direct correlation between amounts of LFA-1 protein expression and both C3 induction and IFN-γ secretion upon activation of their respective T cells (Figure 6F). However, whilst IL-17 production correlated negatively with IFN-γ protein secreted by healthy donor T cells, this correlation was lost in T cells from the patients (Figure S6G).

We were also able to assess monocytes and $CD8^+$ T cells of two patients with LAD-1. These cells were also low in C3, commensurate with deficient LFA-1 expression (Figures S6H-I). In line with $CD4^+$ T cells, both LAD-1 monocytes and LAD-1 $CD8^+$ T cells demonstrated blunted effector function, notably impaired IL-1β (but not IL-6 and TNF) from monocytes and reduced production of cytokines and cytotoxic factors in $CD8^+$ T cells (Figures S6H-I).

We next determined whether impaired immune function in LAD-1 could be rescued by restoration of intracellular C3 or processed C3a. Since this is technically challenging and of low efficiency, and we had limited patient material, we used several methods and selected $CD4^+$ T cells to study. We electroporated cells with intact C3 protein (as $C3H_2O$, which has previously been shown to provide approximately 10% of intracellular C3 in *in vitro* cultures (Elvington et al., 2017)) or adenovirally-delivered C3a or electroporated cells with mRNA encoding C3a, each in conjunction with activation with anti-CD3 and anti-CD46 stimulation (which mimics autocrine C3b generation). We observed that delivery of C3 or C3a, irrespective of the method, proportionally rescued IFN-γ secretion and reduced IL-17 production in patient cells (Figures 6G and S6J-O). The magnitude of IFN-γ rescue was proportional to the degree of LFA-1 deficiency, being greatest in patients 1 and 2, who displayed the lowest LFA-1, C3 and IFN-γ expression prior to C3a reconstitution (Figure 6E). Of note, activating T cells from patients with LAD-1 disease in media containing human serum did not alter IFN-γ production (not shown) and supplementation of C3a into culture medium also failed to rescue IFN-γ production (Figure S6M), demonstrating that exogenous C3 provision by serum did not compensate for lack of the ability to increase intracellular/autocrine C3 expression needed for Th1 induction.

Taken together these data confirmed the *in vivo* requirement for ICAM-1–LFA-1 interactions in inducing sufficient intracellular C3 for Th1 specification and indicate that the

long-known but mechanistically poorly understood Th1 deficiency in LAD-1 is, at least in part, based on defective *C3* gene expression.

Discussion

The complement system has been traditionally viewed as a liver-derived system operating in the extracellular space to direct killing of invading pathogens and regulate (innate) immune cells (Ricklin et al., 2010). Recent work has, however, demonstrated the unexpected existence of an intracellular, autocrine, complement system, the complosome, in human T cells with non-canonical activities (Liszewski et al., 2013). The complosome is fundamentally important for normal human T cell biology via regulation of basic physiological pathways of the cell (Arbore et al., 2016; Liszewski et al., 2013). Specifically, autocrine engagement of the C3aR, CD46, and C5aR1 on $CD4^+$ T cells by C3a, C3b, and C5a generated intracellularly drive homeostatic survival but also the immunometabolic adaptions required for the optimal induction of Th1 and CTL effector function (Arbore et al., 2016; Hess and Kemper, 2016; Kolev et al., 2015; Kolev et al., 2014; West et al., 2018). Although intrinsic intracellular complement was discovered and is still best researched in human T cells, there is growing evidence that this system exists in other cells and is of broad significance. For example, intracellular C3 in pancreatic β-cells regulates autophagy and prevents stress-induced β-cell death (King et al., 2019) and C3b in epithelial cells induces mitochondrial anti-viral signaling protein-dependent pro-inflammatory cytokines upon viral infection (Tam et al., 2014). Thus, normal C3 and C5 activity within (immune) cells is critical to health and our lack of insight into how the complosome is regulated currently hampers therapeutic modulation of this system.

T cells in *ex vivo* culture can 'ingest' small amounts of the spontaneously hydrolyzed form of complement C3, $C3H_2O$, from media to sustain survival (Elvington et al., 2017) but these amounts do not support induction of Th1 effector function. However, external C3 is only minimally present in in lymph nodes and peripheral tissues where antigenic challenge occurs. Thus, an alternative mechanism of intracellular C3 generation must be operative at these sites to support tissue immunity. Here, we have identified the integrin LFA-1 as the key inducer of cell-intrinsic *C3* gene transcription in a range of key human immune cells, including myeloid cells and $CD4^+$ and $CD8^+$ T lymphocytes. We have also delineated the LFA-1-C3 axis in more detail for $CD4^+$ T cells: LFA-1 engagement on $CD4^+$ T cells (resting T cells express a pool of extended headpiece-activated LFA-1 (Feigelson et al., 2010)) via ICAM-1, on endothelial cells during diapedesis or cognate APC-T cell interaction during priming, drove

T cell *C3* gene expression. The provision of an appropriately timed TCR signal (e.g. via TCR-MHC-peptide complexes) then triggered CTSL–mediated increased intracellular processing of C3 into C3a and C3b. Secretion of these fragments into the extracellular space then results in autocrine engagement of C3aR and CD46 and acquisition of Th1 and optimal CTL effector function. Of note, LFA-1-mediated C3 expression (mRNA transcription and protein amounts) is sustained for about 12h in the absence of concurrent TCR stimulation. This scenario provides naive (and central memory) T cells that (re)transmigrate through the high endothelial venules with a source of survival-sustaining C3 (Liszewski et al., 2013) and thus time to scan APCs in the lymph nodes for cognate antigen. Similarly, effector memory T cells, which circulate in the periphery and survey peripheral tissue in search of 'dangerous' antigens would also be 'pre-loaded' with ample C3 in non-inflamed tissue and can hence respond rapidly in the event of pathogen re-encounter (Jameson and Masopust, 2018). Our data showed that LFA-1 also regulated intrinsic *C3* expression and effector function in myeloid cells. This observation aligns well with the long-known fact that myeloid cells are major producers of extra-hepatic C3 (Lubbers et al., 2017) and that monocytes/macrophages from serum C3 deficient patients fail to develop into normally functioning dendritic cells (Ghannam et al., 2008).

The biological importance of LFA-1-mediated C3 expression is underpinned by our finding that defective Th1 and CTL responses and IL-1β secretion by monocytes in patients with LAD-1 correlated with proportional reductions in C3 expression, and could be corrected proportionally by restoring intracellular C3 protein amounts, demonstrated in principle utilizing $CD4^+$ T cells. Of note, the patients' cells had low amounts of mRNAs encoding *C3* and reduced C3a activation fragment generation and were able to sustain homeostatic survival. They failed, however, to induce the increased amount of C3 protein needed for induction of appropriate cellular effector functions. It is currently unclear whether LFA-1-independent signals sustain basal amounts of *C3* gene expression in immune cells. In addition, it is highly likely that additional incoming signals, aside from LFA-1, either received during diapedesis or once the cells are in the tissue, will impact on C3 protein amounts. Although immune cells can ingest exogenous $C3H_2O$ *in vitro*, this has not yet been demonstrated *in vivo* (Elvington et al., 2017). Moreover, immune cells only utilize about 10% of such exogenously sourced $C3H_2O$ for intracellular C3a generation and expel the remaining non-cleaved 90% rapidly

(Elvington et al., 2017). This could indicate that endogenously generated C3 is localized to and activated within specific cellular sub-compartments, which are distinct from those of the C3 'uptake route'. It may also explain why over-expression of C3 or C3a by viral delivery or electroporation in LAD-1 patient cells was inefficient, namely that C3a had a short half-life (it is degraded very rapidly by carboxypetidases into inactive C3a-desArg) and was not efficiently targeted to its intracellular receptor in lysosomal compartments. Thus, the rescue of IFN-γ production in patient cells was likely to be proportional to the degree of C3 or C3a over-expression that can be achieved.

The impaired ability of $CD4^+$ T cells from patients with LAD-1 to generate IFN-γ was previously thought to be rooted in muted TCR signaling (Abraham et al., 1999; Chirathaworn et al., 2002; Hogg et al., 2011; Varga et al., 2010), failure of optimal pSMAC formation during T cell priming (Monks et al., 1998), and/or reduction in Th1-driving Notch activity on $CD4^+$ T cells (Verma et al., 2016), events which are all regulated by LFA-1. Our data here suggest that it is the inability of LAD-1 T cells to generate sufficient intracellular C3 and subsequent autocrine CD46 engagement that is the major contributor to their Th1 defect. This notion is supported by the fact that CD46 ligand binding *per se* mimics key functions of LFA-1 during T cell activation: CD46-mediated signals synergize with TCR to activate cellular kinases (Astier et al., 2000; Kemper and Atkinson, 2007; Kolev et al., 2015) and CD46 is required for Notch-1 and Jagged-1 upregulation in human $CD4^+$ T cells (Le Friec et al., 2012). In addition, $CD4^+$ T cells from CD46-deficient patients, similar to those from patients with LAD-1, proliferate normally, and generate functional Th2 and Th17 cells (Le Friec et al., 2012). Likewise, we observed that LFA-1 engagement on $CD4^+$ T cells parallels the metabolic changes previously observed upon direct CD46 co-stimulation, including activation of mTORC1, glycolysis and OXPHOS.

These observations established a functionally critical role for the integrin network as key regulators of intracellular complement activity. We had previously demonstrated that both increased intracellular C3 and its processing contribute to the Th1 hyperactivity observed in patients with autoimmune arthritis and that pharmacological targeting of the C3 complosome was ameliorative (Cardone et al., 2010). The current study suggests that the hyper-C3 expression in immune cells from patients with RA may potentially be driven by LFA-1

engagement during movement of cells into sites of inflammation. Moreover, we found that expression of *C3* by T cells at these sites may represent a biomarker of the severity of RA.

Finally, several observations made during our study suggest to us that the LFA-1-regulated activity of the complosome may go beyond induction of immune cell effector function. ICAM-1-LFA-1 interaction is also required for normal central T cell memory formation (Badell et al., 2010; Parameswaran et al., 2005) and retention of tissue-resident memory T cell pools after infections (McNamara et al., 2017; Thatte et al., 2003). These facts, together with the unexpected finding that a defining characteristic of immune cells isolated from tissues is the expression of a virtually complete intracellular complement system, including all key components, regulators and receptors, indicate that the complosome may also play a role in T cell memory and/or the maintenance of T cell tissue residency. The recurrent viral infections in patients with CD46 deficiency support this notion (Arbore et al., 2018; Le Friec et al., 2012). Similarly, our finding that glycolysis and OXPHOS were differently affected by LFA-1 and CD46 engagement in naive and memory T cells suggests that the LFA-1-C3 axis directs the distinct metabolic programs that characterize these T cell subpopulations (Buck et al., 2017; van der Windt and Pearce, 2012). We are therefore currently actively pursuing defining whether intrinsic C3 and/or C5 is also required for T cell memory development and/or immune cell tissue residency. However, as discussed, CD46, the major 'target' for intrinsic C3b generation in human cells, is not expressed in mice and the intracellular processing of C3 in mouse immune cells requires a distinct, yet unidentified, mechanism. Furthermore, the presence or expression pattern of the anaphylatoxin receptors on mouse $CD4^+$ and $CD8^+$ T cells is a matter of controversy in the field (Laumonnier et al., 2017) as is the dependency of murine Th1 induction on T cell-intrinsic C3 and/or C5 production (Heeger and Kemper, 2011). Thus, there are substantial species-specific differences as to how humans and mice engage and regulate the complosome for immunity. Therefore, the C3 reporter mice generated here will be a valuable tool to detect *in vivo* C3 induction broadly, but the specific molecular induction pathways queried should be carefully evaluated for transferability to humans.

In summary, we identified expression of complement components, including C3, as one of the defining features of immune cells in tissues, with LFA-1-mediated 'C3 licensing' representing a biological pathway of broad significance to multiple immune cell subsets. Perturbations of this pathway contribute to both immunodeficiency (LAD-1 disease) and the

severity of autoimmunity (RA). These findings align well with the emerging role of the complosome as a central contributor to general (immune) cell homeostasis and functional activity in health and disease.

Acknowledgements

We thank the patients and the healthy donors for their support. This work was financed by the MRC Centre grant MR/J006742/1, an EU-funded Innovative Medicines Initiative BTCURE (C.K.), a Wellcome Trust Investigator Award (grant 102932/Z/13/Z to C.K), a Wellcome Trust Intermediate Clinical Fellowship (grant 097261/Z/11/Z to B.A.), the National Heart, Lung, and Blood Institute of the NIH (grant 5K22HL125593 to M.Kaz), a grant from the Guy's and St Thomas' Charity (C.K., and B.A.), the National Institute for Health Research (NIHR) Biomedical Research Centre at Great Ormond Street NHS Foundation Trust (L.R.W. and L.R.), The King's College London BRC Genomics Facility, the National Institute for Health Research (NIHR) Biomedical Research Centre based at Guy's and St Thomas' NHS Foundation Trust and King's College London, SNSF funding to C.H. (31003A_172848), and [in part] by the Intramural Research Program of the NIH, the National Institute of Diabetes and Digestive and Kidney Diseases (project number ZIA/DK075149 to B.A.) and the National Heart, Lung, and Blood Institute (project number ZIA/HL006223 to C.K.).

Author contributions

Conceptualization: M.Kol., E.E.W., M.Kaz., B.A., and C.K.; Methodology: M.Kol., E.E.W., E.A.M., D.McG., B.A., M.Kaz., and C.K.; Formal Analysis: A.E.M., L.W., N.M.M., M.J.K., S.M.H., P.L., M.Kaz., and B.A.; Investigation: M.Kol., E.E.W., N.K., D.C., E.A.M., J.R., T.F., M.L.B., J.L., S.D., E.C.R., K.D.M-B., A.B., P.L, N.M.M., C.H., B.A., and C.K. Resources: L.R.W., A.C., M.J.K., N.M.M., and S.M.H.; Writing – Original Draft: M.Kol., E.E.W., M.Kaz., B.A., and C.K.; Writing – Review & Editing: all authors; Supervision: C.H., M.Kaz., B.A., and C.K.; Funding Acquisition: L.R.W., L.R., C.H., M.Kaz., B.A., and C.K.

Declaration of interests

The authors declare no competing interests.

Figure legends

Figure 1: Complement *C3* gene transcription is a feature of immune cells in tissues. (**A-C**) Significantly enriched canonical pathways by GSEA comparing transcriptomes of human $CD4^+$ (**A**) and $CD8^+$ T cells (**B**) isolated from lung versus spleen (data from GSE94964) and monocytes and macrophages (**C**) isolated from tissues versus blood (data from GSE117970). Left, pathways ranked by significance (false-discovery rate q-values), with complement pathways highlighted in red and integrin pathways in yellow. Right, GSEA plots for the top complement pathways in **A-C,** respectively. (**D-F**) Expression of *C3* mRNA in $CD4^+$ (**D**) and $CD8^+$ (**E**) T cells isolated from lung versus spleen (data from GSE94964) and monocytes and macrophages (**F**) isolated from tissues versus blood (data from GSE117970). (**G**) Schematic depicting the methicillin-resistant *Staphylococcus aureus* (MRSA) ear infection model. Wild type (WT) or *C3*-Td Tomato reporter mice (C3-TdT) were infected in the ear followed by intravital microscopy and blood and organ harvest at day 7 post-infection. (**H**) Still capture of an intravital imaging movie (see **Movie S1**) of an MRSA-infected ear section of a WT (left) and C3-TdT reporter mouse (right) at day 7 post-infection. Bar, 30 μm. (**I**) Representative FACS analysis (top) and cumulative data (below) showing Td Tomato reporter activity in $CD4^+$ (n=7) and $CD8^+$ (n=5) T cells of WT and C3-TdT mice from different tissues at day 7. (**J**) Representative FACS analysis (left) and cumulative data (right) showing Td Tomato reporter activity in tissue macrophages of WT and C3-TdT mice from the site of infection at day 7 (n=5). **I-J** show cumulative data from 3-5 experiments. Bars show mean + SEM. * $p<0.05$, ** $p<0.01$, *** $p < 0.001$, **** $p < 0.0001$. See also **Figure S1 and Table S1**.

Figure 2: ICAM-1 is a key driver of *C3* gene transcription in $CD4^+$ T cells. (**A**) Schematic depicting the integrins and selectins (with respective binding partners in parentheses) involved in rolling, adhesion and transmigration assessed for C3-dependent Th1 induction. (**B**) Reporter activity of splenic $CD4^+$ T cells from the *C3*-Td tomato reporter mouse activated with antibodies to CD3 or CD3+CD28 with or without increasing concentrations of immobilized ICAM-1 for seven days and *C3*-Td Tomato signal measured by flow cytometry. Shown are cumulative data from n=5 independent experiments. (**C**) *C3* mRNA (above) and protein (below) expression over time in healthy donor naive and memory $CD4^+$ T cells cultured in the presence or absence of ICAM-1 alone. Cumulative data (mean ± SEM; n=3 independent experiments); both the *C3* mRNA and protein expression curves are higher for both memory and naive cells with ICAM-1 compared to without ICAM-1 ($p<0.001$ for mRNA expression in both cell types; $p<0.0001$ for C3 protein in naive T cells and $p<0.01$ for C3 protein in memory T cells). (**D-E**) Confocal images for *C3* mRNA (using the PrimeFlow assay) and IFN-γ protein (**D**) and flow cytometry histograms for *C3* mRNA (PrimeFlow assay) (**E**) in bulk $CD4^+$ T cells activated for 36h in the presence and absence of ICAM-1. Shown are representative examples of four independent experiments (n=4). Size bar in 'D', 2 μm. Bars show mean + SEM throughout. * $p < 0.05$, ** $p < 0.01$, **** $p < 0.0001$. See also **Figure S2.**

Figure 3. ICAM-1–LFA-1 interaction during diapedesis is required for *C3* gene transcription. (**A**) Schematic representation of the *in vitro* transmigration assay utilizing a trans-well system with HUVEC cells and sorted naive and memory $CD4^+$ T cells. (**B-D**) Transmigration (**B**) of healthy donor naïve and memory $CD4^+$ T cells across a trans-well

system in the presence and absence of IL-1β (induces ICAM-1 expression by HUVEC cells), with and without DEL-1 (a specific inhibitor of LFA-1/ICAM-1 interaction) and expression of *C3* (**C**) and *IFNG* (**D**) mRNA by transmigrated cells. Cumulative data from n=6-9 independent experiments. Bars show mean ± SEM. *$p < 0.05$, **$p < 0.01$, ***$p < 0.005$. See also **Figure S3**.

Figure 4: ICAM-1 drives C3-dependent metabolic reprogramming during T cell activation. (**A**) IFN-γ secretion (left) and intracellular C3a generation (right) by healthy donor $CD4^+$ T cells activated as shown in the presence and absence of ICAM-1 with and without a cell-permeable cathepsin L inhibitor (CTSLi) for 72h (n=4 independent experiments). (**B**) Representative flow cytometry plots from n=4 independent experiments showing *C3* mRNA and the mTOR down-stream target S6 kinase phosphorylated at ser235/ser236 (p-S6) in healthy donor $CD4^+$ T cells activated as shown in the presence or absence of ICAM-1 for 36h. (**C**) Extracellular acidification rate (ECAR, a measure of glycolysis) and oxygen consumption rate (OCR, a measure of oxidative phosphorylation) in healthy donor naive $CD4^+$ T cells activated as shown in the presence or absence of ICAM-1 with and without a CTSL inhibitor for 36h. Shown are representative ECAR (above) and OCR (middle) graphs together with cumulative data of the maximal respiration and glycolysis (below) from n=3 independent experiments. NA, non-activated; FCCP, *p*-trifluoromethoxyphenyl hydrazone; OM, oligomycin; ROT, rotenone. Bars show mean ± SEM. *$p < 0.05$, **$p < 0.01$, ***$p < 0.005$, ****$p < 0.001$. See also **Figure S4**.

Figure 5: LFA-1 induces *C3* gene expression in $CD4^+$ T cells via AP-1. (A-D) *C3* mRNA expression in naive (**A** and **B**) and memory (**C** and **D**) $CD4^+$ T cells activated as indicated in the presence or absence of ICAM-1 with and without a cell-permeable AP-1 inhibitor (AP-1 inh.) or DMSO carrier control at 72h post activation. Shown are representative flow cytometry histograms of (**A** and **C**) and cumulative data from n=5 (**B**) and n=4 (**D**) independent experiments**.** NA, non-activated. Error bars represent mean + SEM. **$p < 0.01$ ***, $p < 0.005$, ****$p < 0.001$. See also **Figure S5**.

Figure 6: LAD-1 disease causes failure of C3 expression and Th1 induction. (**A**) Steady-state expression of *C3* and *IFNG* mRNA in paired $CD4^+$ T cells drawn from blood and synovial fluid of pediatric patients with juvenile idiopathic oligo-arthritis (n=4; Table S2). Bars show mean + SEM. (**B**) IFN-γ secretion by paired $CD4^+$ T cells drawn from blood and synovial fluid of two patients with rheumatoid arthritis (RA) activated *in vitro* with antibodies against CD3 with, or without, ICAM-1. (**C-D**) *C3* mRNA expression by synovial T cells of patients with either oligo-arthritis (OA), non-inflamed RA or inflamed RA derived from an independent dataset (Zhang et al., 2019) (**C**) and receiver operating characteristic curves showing performance of *C3* and *IFNG* mRNA expression in synovial T cells as biomarkers to distinguish inflamed from un-inflamed RA (**D**). (**E**) LFA-1 expression (top), *C3* mRNA (middle) and IFN-γ secretion (bottom) by peripheral blood $CD4^+$ T cells from patients with LFA-1 mutations (LAD-1 disease) (see Table S3) and age- and sex-matched controls activated *in vitro* as shown with, and without ICAM-1 for 72h. Data are from three patients, two of whom donated twice, and five controls. Bars represent mean of duplicate measurements per subject. (**F**) regression lines showing correlation between IFN-γ and LFA-1 expression (left) and between *C3* mRNA and LFA-1 expression (right) from primary data in (**E**). 95% confidence intervals of the regression

line are shown and individual donors are marked. (**G**) IFN-γ secretion by peripheral blood $CD4^+$ T cells from three patients with LAD-1 disease after transduction with control adenovirus or adenovirus encoding C3a, electroporation with mRNA encoding GFP or C3a or electroporation with BSA or $C3H_2O$ protein, as indicated. Cells were activated with anti-CD3+CD46+ICAM-1 after transduction or electroporation. Each patient has been labelled, two of whom donated three times, and the over-expression method shown by color-coding. *p<0.05. See also **Figure S6 and Tables S2 and S3**.

STAR Methods

KEY RESOURCES TABLE

REAGENT or RESOURCE	SOURCE	IDENTIFIER
Antibodies		
Anti-human CD3 (OKT-3)	Washington University Hybridoma Center	RRID:AB_2619696
Anti-human CD28 (CD28.2)	BD Biosciences	Cat. #555728, RRID:AB_396071
Anti-mouse CD3 (145-2C11)	BD Biosciences	Cat. #553058, RRID:AB_394591
Anti-mouse CD28 (37.51)	BD Biosciences	Cat. #553295, RRID:AB_394764
Anti-human CD46 (TRA-2-10)	Washington University Hybridoma Center (WUHC)	Clone TRA-2-10, (Wang et al., 2000), RRID:AB_10895912
Anti-human C3	Abcam	Cat. #ab196639, RRID:AB_10572686
Anti-human C3a/C3adesArg (2991)	Abcam	Cat. #ab11873, RRID:AB_298655
Anti-human p-S6 (N7-458)	BD Biosciences	Cat. #561457, RRID:AB_10643763
Anti-human CD45RA Pe/Cy7 (HI100)	Biolegend	Cat. #304126, RRID:AB_10708879
Anti-human CD45RO Brilliant violet 711 (UCHL1)	Biolegend	Cat. #304236, RRID:AB_2562107
Anti-human CD197 Brilliant Violet 605 (CCR7) (G043H7)	Biolegend	Cat. #353232, RRID:AB_2563866
Anti-human CD11a- Alexa Fluor 488 (m24)	Biolegend	Cat. #363404, RRID:AB_2565289
Anti-human CD11a Alexa Fluor 488 (HI111)	Biolegend	Cat. #301216, RRID:AB_2265103
Anti-human CD11a Alexa Flour 647 (HI111)	Biolegend	Cat. #301218, RRID:AB_2128991
Anti-human CD54 Pacific Blue (ICAM-1) (HCD54)	Biolegend	Cat. #322716, RRID:AB_893384
Anti-human CD107a (H4A3)	Biolegend	Cat. #328638, RRID:AB_2565838
Anti-human Granzyme B (GB11)	Biologend	Cat. #511405, RRID:AB_2243896
Anti-human LFA-1 (R7.1)	Thermo Fisher Scientific	Cat. #BMS102, RRID:AB_187708
Anti-human CD18 Pe/Cy7 (TS1/18)	Biolegend	Cat. #302118, RRID:AB_2565585
Anti-human CD18 (Ts/18)	Biolegend	Cat. #302102, RRID:AB_314220
Anti-human CD3 Pacific Blue (OKT4)	Biolegend	Cat. #317429, RRID:AB_1595438
Anti-human INF-γ FITC (B27)	Biolegend	Cat. #506504, RRID:AB_315437

Anti-human C3a/C3a-desArg (D17/1)	Biolegend	Cat. #518002, RRID:AB_10895750
Anti-human cFOS (9FS)	Cell Signalling	Cat. #2250S, RRID:AB_2247211
Anti-human HSP70 (B-6)	Santa Cruz Biotechnology	Cat. #sc-7298, RRID:AB_627761
Anti-mouse IgG Alexa Fluor 488 (polyclonal)	Molecular Probes/Thermo Fisher	Cat. #A11001, RRID:AB_2534069
Anti-mouse CD4 PE (RM4-5)	Biolegend	Cat. #100512, RRID:AB_312715
Anti-mouse CD4 PacBlue (RM4-5)	Biolegend	Cat. #100531, RRID:AB_493374
Anti-mouse CD25 APC (PC61)	Biolegend	Cat. #102012, RRID:AB_312861
Anti-mouse CD45RB FITC (C363-16A)	Biolegend	Cat. #103306, RRID:AB_313013
Anti-mouse CD90.2 PerCP-Cyanine5.5 (Thy2.1) (53-2.1)	Biolegend	Cat. #140322, RRID:AB_2562696
Anti-mouse IFN-γ Alexa Fluor 488 (XMG1.2)	Biolegend	Cat. #505813, RRID:AB_493312
Anti-mouse IL-17A PE (TC11-18H10.1)	Biolegend	Cat. #506922, RRID:AB_2125010
Anti-Rabbit F(ab')^2 fragment RPE	Molecular Probes/Thermo Fisher	Cat. #A10542, RRID:AB_1500781
IRDye 680RD Goat anti-Mouse IgG Secondary Antibody	LI-COR Biosciences	Cat. #926-68070, RRID:AB_10956588
IRDye 800CW Goat anti-Rabbit IgG Secondary Antibody	LI-COR Biosciences	Cat. #926-32211, RRID:AB_621843
Bacterial and Virus Strains		
Adenovirus containing C3a portion of C3	In house generated	N/A
Control Adenovirus	In house generated	N/A
Methicillin-resistant *Staphylococcus aureus*	USA300 clinical isolate	Cat. #FPR3757
Biological Samples		
Healthy donor blood buffy coats	NHSBT (UK)	N/A
Healthy donor blood buffy coats	NIH Blood Bank (NIH)	N/A
Healthy donor freshly drawn blood	King's College London or Medical Center at National Institutes of Health	N/A
Blood samples from adult CD11a/CD18-deficient patients with lymphocyte adhesion deficiency (LAD)-1 syndrome	Medical Center in National Institutes of Health	N/A
Blood and synovial fluid from adult patients suffering from Rheumatoid Arthritis	King's College London	N/A
T cells isolated from Floxed C3 IRES-tdTomato or C3 KO mice	genOway and NIH	N/A
Chemicals, Peptides, and Recombinant Proteins		
Human ICAM-1-Fc chimera	Biolegend	Cat. #552906
Mouse ICAM-1-Fc chimera	Biolegend	Cat. #553006
Recombinant human MU E-selectin (CD62E) Fc chimera	Biolegend	Cat. #755504
Human recombinant VCAM-1	Peprotech	Cat. #150-04

Human recombinant PECAM1, tagged with hIgG1	Life Technologies	Cat. #10148-H02H-50
Human recombinant CD99	Abnova	Cat. #H00004267-P01
Human recombinant EDIL3 (DEL1)	Abnova	Cat. #H00010085-P01
Purified human C3	CompTech	Cat. #A113
Purified human iC3b	CompTech	Cat. #A115
Purified human C3a	CompTech	Cat. #A118
Recombinant Human CCL1 (I-309)	Biolegend	Cat. #582704
Recombinant Human CXCL3 (GRO-γ)	Biolegend	Cat. #586304
Recombinant Human CCL5 (RANTES)	Biolegend	Cat. #580204
Recombinant Human CXCL10 (IP-10)	Biolegend	Cat. #573504
Recombinant Human CCL20 (MIP-3α)	Biolegend	Cat. #583804
c-Fos inhibitor (T5224)	BioVision	Cat. #9546-5
Recombinant human IL-2	Present from C. Pham, Washington University, STL	N/A
Recombinant human IL-1β	Biolegend	Cat. #579404
LPS from *Salmonella minnesota*	Sigma Aldrich	Cat. #L7011
LIVE/DEAD Fixable Near-IR Dead Cell Stain Kit	Thermo Fisher Scientific	Cat. #L34976
LIVE/DEAD™ Fixable Aqua Dead Cell Stain Kit	Thermo Fisher Scientific	Cat. #L34965
Tryptic Soy Broth	Thermo Fisher Scientific	Cat. #112641
Liberase TL	Roche Diagnostic Corp.	Cat. #05401160001
Critical Commercial Assays		
Negative EasySep Human CD T Cell Isolation Kit	Stemcell Technologies	Cat. #17591
RosetteSep Human CD4 T Cell Enrichment Kit	Stemcell Technologies	Cat. #15062
EasySep Human Naïve CD4 T Cell Isolation Kit	Stemcell Technologies	Cat. #19555
Human CD8 T Cell Isolation Kit	Miltenyi Biotec	Cat. #130-096-495
Human CD14 MicroBeads	Miltenyi Biotech	Cat. #130-050-201
EasySep Mouse CD4 T cell Isolation Kit	Stemcell Technologies	Cat. #19752
Human Th1/Th2/Th17 Cytokine Bead Array	BD Biosciences	Cat. #560484
LEGENDplex™ Human Th Panel (13-plex)	Biolegend	Cat. #740722
Human IL-1 beta/IL-1F2 Quantikine ELISA KIT	R&D Systems	Cat. #DLB50
LEGENDplex™ Mouse Th Cytokine Panel (13-plex)	Biolegend	Cat. #740741
Human PrimeFlow RNA Kit	eBioscience/Thermo Fisher Scientific	Cat. #88-18005-210
Direct-zol RNA Mini Prep Kit	Zymo Research	Cat. #R2052
BD Cytofix/Cytoperm™ Fixation/Permeabilization Kit	BD Biosciences	Cat. #554714
Pacific Blue™ Protein Labeling Kit	Thermo Fisher Scientific	Cat. #P30012
TaqMan Gene Expression Master Mix	Thermo Fisher Scientific	Cat. #4369016
RNAqueous™ Micro Total RNA Isolation Kit	Thermo Fisher Scientific	Cat. #AM1931
High Capacity cDNA Reverse Transcription Kit	Applied Biosystems	Cat. #4368814
Protoscrip II	New England Biolabs	Cat. #M0368S

RNAqueous-Micro Total RNA Isolation Kit	Thermo Fisher Scientific	Cat. #AM1931
Experimental Models: Cell Lines		
Human umbilical cord vein epithelial cells (HUVEC)	Thermo Fisher Scientific	Cat. #C0035C
Experimental Models: Organisms/Strains		
C3$^{IRES\text{-}tdTomato}$ C57BL/6 mice	Genoway, this study	N/A
Rag2$^{-/-}$ *C57BL/10 mice*	Taconic	Rag2 – Model 758
Cre Deleter mice C57BL/6	Taconic, NIH facility	Cre Deleter Model
Oligonucleotides		
C3 Primer Set	Applied Biosystems	Hs00163811_m11, Cat. #1615290
18s Control rRNA	Applied Biosystems	Cat. #4318839
C3 type 1 Probe Set	eBioscience/Thermo Fisher Scientific	Cat. #PF-210, assay ID VA1-12373-PF
FAM c-FOS TaqMan Probe	Thermo Fisher Scientific	Hs00170630_m1
FAM 18s TaqMan Probe	Thermo Fisher Scientific	Hs99999901_s1
Synthesized C3a mRNA	Trilink	N/A
Synthesized eGFP mRNA	Trilink	N/A
Software and Algorithms		
Prism Versions 7 and 8	GraphPad	N/A
FlowJo 9 or 10	FlowJo	https://www.flowjo.com
Image Studio v5.2	LI-COR Biosciences	https://www.licor.com
Legendplex v8.0	Biolegend	Legendplex v8.0
Critical equipment		
MaxCyte ATx Transfection System	MaxCyte	N/A
Odyssey CLx Imaging System	LI-COR Biosciences	N/A
Attune NXT Flow Cytometer	Thermo Fisher Scientific	N/A
BD FACSCanto™ II Flow Cytometer	BD Biosciences	N/A
LSRFortessa™ Flow Cytometer	BD Biosciences	N/A
Seahorse XF-96 Metabolic Extracellular Flux Analyzer	Seahorse Bioscience	N/A
Confocal Microscope A1R SI	Nikon	N/A
C1000 Touch™ Thermo Cycler with CFX96 Optical Reaction Module	Bio-Rad	N/A
Criterion™ System for Western Blotting	Bio-Rad	N/A
Medimachine System Homogenizer	BD Biosciences	N/A
SP8 Two Photon Microscope (Nikon) with Mai Tai HP DeepSee Laser and Insight DS Laser (both Spectra-Physics)	Leica, Spectra-Physics	N/A

LEAD CONTACT AND MATERIALS AVAILABILITY

The *C3*$^{IRES\text{-}tdTomato}$ C57BL/6 mice generated in this study will be available upon request. Further information and requests for resources and reagents should be directed to and will be fulfilled by the corresponding Lead Contact, Claudia Kemper (claudia.kemper@nih.gov).

EXPERIMENTAL MODEL AND SUBJECT DETAILS

Healthy donors and patients

Blood samples were obtained and processed with appropriate ethical and institutional approvals (Wandsworth Research Ethics Committee, REC number 09/H0803/154; Bloomsbury Research Ethics Committee, REC number 95RU04, the Clinic of the National Institute of Allergy and Infectious Diseases (NIAID) and NIAMS/NIDDK IRB (IRB 01-AR-0227). All healthy donors and patients gave informed consent prior to sample collection. In all, data from 13 female healthy donors (aged 22, 23, 26, 28, 32, 32, 38, 45, 46, 46, 54, 62, and 66 years), and 12 male donors (aged 22, 26, 29, 34, 38, 42, 42, 45, 45, 48, 59, and 66 years) were used in this study. Immune cells (monocytes and $CD4^+$ and $CD8^+$ T cells) were purified from freshly drawn blood or from buffy coats (NHSBT, Tooting, UK and NIH Blood Bank, Bethesda, USA) and activated as described in Method Details. Two adult patients (one female, aged 22 years, and one male, aged 42 years) with rheumatoid arthritis (RA) according to ACR criteria and four patients with juvenile idiopathic oligo-arthritis (JIA) were recruited to the study (3 females and 1 male). Both RA patients had active disease in spite of therapy with combination disease modifying anti-rheumatic drugs methotrexate. Detailed information on the JIA patients is provided in **Table S2**. Synovial fluid was obtained during therapeutic knee joint arthrocentesis. Three adult patients (one female, aged 23 years, and two males, aged 22 and 23 years) with mutations in *ITGB2* (encodes the common CD18 subunit of the β2 integrins) and lymphocyte adhesion deficiency syndrome (LAD-I) were assessed and treated at the NIAID Clinic (Moutsopoulos et al., 2017). Clinical information on the LAD-1 patients is provided in **Table S3**.

Mice

Floxed C3 IRES-tdTomato reporter mice on a C57BL/6 background were generated by genOway via knock-in insertion of an 'internal ribosome entry site (IRES)-tdTomato cassette' after the stop codon of the *C3* gene which preserved the 5' and 3' UTR regulatory elements and hence physiological C3 expression and activity. The *C3* gene region was isolated from C57BL/6N mouse genomic DNA and inserted into a targeting vector that allowed for

diphtheria toxin-mediated negative and neomycin-mediated positive selection of the transfected isogenic ES cell line. Selected clones were screened via PCR and Southern blotting for successful 5' and 3' homologous recombination. Validated ES cells were injected into blastocysts which were implanted into foster mothers. Resulting chimeric mice were bred to full homozygosity of the C3-IRES-tdTomato knock-in region, wild type litter mates were used as control animals in all experiments, and equal numbers of male and female animals were used in this study. To generate C3 deficient animals, the floxed C3 IRES-tdTomato reporter mice were breed to Cre-Deleter mice (Taconic, NIH animal facility) of the same background. The C57BL/10 *Rag2*$^{-/-}$ mice were obtained from Taconic. All animals were maintained in AALAC-accredited BSL2 facilities at the NIH and experiments performed in compliance with an animal study proposal approved by the NHLBI Animal Care and Use Committee. A schematic of the inserted cassette and data on ES clone selection of the *C3* IRES-tdTomato reporter mice are provided in Figure S1E-H.

METHOD DETAILS

Antibodies, Proteins and Inhibitors

Antibodies for mouse T cell stimulation (anti-mouse CD3 (145-2C11) and anti-mouse CD28 (37.51)) as well as anti-human CD28 (CD28.8) were bought from BD Biosciences (San Diego, CA). Antibodies to human CD3 (OKT-3) and CD46 (TRA-2-10) used for human T cell stimulation were purified in-house from hybridoma cell lines (Wang et al., 2000). Monoclonal antibodies to human C3 (EPR2988) and the neo-epitope C3a/C3adesArg (2991) were purchased from Abcam (Cambridge, UK). The antibody recognizing human p-S6 (N7-458) was purchased from BD Biosciences, whilst antibodies to human CD45RA PE/Cy7 (HI100), CD45RO Brilliant violet 711 (UCHL1), CD197/CCR7 Brilliant Violet 605 (G043H7), CD11a Alexa Fluor 488 (m24), CD11a Alexa Fluor 488 (HI111), CD11a Alexa Flour 647 (HI111), CD54/ICAM-1 Pacific Blue (HCD54), CD18 Pe/Cy7 (TS1/18), CD3 Pacific Blue (OKT4), INF-γ FITC (B27), and to C3/C3a/C3a-desArg (D17/1) were all purchased from Biolegend (San Diego, CA). Anti-human CD107 Brilliant Violet 650 (H4A3) and anti-human granzyme B Alexa Fluor 647 (GB11) were from Biolegend and the function neutralizing anti-human LFA-1 antibody (R7.1) from Thermo Fisher Scientific. Anti-human cFOS (9FS) was bought from Cell Signaling Technology (Danvers, Massachusetts). The following anti-mouse antigen

antibodies were bought from Biolegend: IFN-γ Alexa Fluor 488 (XMG1.2), IL17A PE (TC11-18H10.1), CD4 PacBlue (RMA-5), CD4 PE (RM4-5), Thy1.2 PerCP-Cy5.5 (53-2.1), CD45RB FITC (C363-16A), and CD25 APC (PC-61). Anti-mouse IgG Alexa Fluor 488 (A11001) and RPE-conjugated anti-Rabbit F(ab')2 fragments (A10542) were obtained from Molecular Probes/Life Sciences (Paisley, UK), and anti-rabbit IgG Brilliant Violet 421 (Poly4064) was from Biolegend. Carrier-free recombinant human ICAM-1-Fc Chimera and carrier-free recombinant mouse Icam-1-Fc Chimera (553006), and recombinant human MU E-selectin/CD62E-Fc Chimera were from Biolegend. Recombinant human VCAM-1 (150-04) was from PeproTech (Rocky Hill, NJ) while recombinant human PECAM-1 tagged with hIgG1-FC was from Thermo Fisher Scientific (Waltham, MA). Recombinant human CD99 (H00004267-P01) and EDIL3/DEL1 (H00010085-P01) proteins were from Abnova Corporation (Taipei, Taiwan). Recombinant human IL-1β (599404) was bought from Biolegend, and LPS (*Salmonella minnesota*) from Sigma-Aldrich (L7011, Saint Louis, MO). Recombinant human CCL1 (582704), CXCL3 (586304), CCL5 (580204), CXCL10 (573504), and CCL20 (583804) were all purchased from Biolegend and used at 1 μg/ml media concentration. Human serum-purified C3 (A113), iC3b (A115), or C3a (A118) were purchased from Complement Technology (Tyler, TX), and human recombinant IL-2 (200-02) was bought from PeproTech. The chemical specific inhibitor of c-FOS/AP-1 (T5224) was provided by BioVision (Milpitas, CA) and used at 1 μM concentration. The cell-permeable inhibitor to cathepsin L (ALX-260-133-M001) was bought from Enzo Life Sciences (Exeter, UK) and used at 50 nM/ml. To monitor for cell viability, the LIVE/DEAD Fixable Near-IR Dead Cell Stain Kit (L34976) or the LIVE/DEAD Fixable Aqua Dead Cell Stain Kit (L34965), both from Thermo Fisher Scientific, were used.

Human $CD4^+$ and $CD8^+$ T cell Purification and *In Vitro* Activation

Human bulk $CD4^+$ or $CD8^+$ T cells were isolated from PBMCs (obtained from freshly drawn blood after centrifugation using Lymphoprep separation medium (Corning, Vienna, VA) using either the MACS Human $CD8^+$ T cell Isolation Kit (130-096-495) from Miltenyi Biotech, (Bergisch Gladbach, Germany), the Negative Selection EasySep CD4 T cell kit (17951) or RosetteSep Human CD4 Cell Isolation Kit (15062) from Stemcell Technologies (Vancouver, Canada) according to the manufacturers' instructions. Purity of isolated bulk T lymphocyte

fractions was typically > 97 %. Purified naïve and/or memory $CD4^+$ T cells were obtained through usage of the EasySep Human Naive $CD4^+$ T Cell Isolation Kit (19555) from Stemcell Technologies (naive $CD4^+$ T cells) or via cell sorting of enriched $CD4^+$ T cells after staining with for 30 min at 4 ^oC with anti-CD4 Pacific Blue, anti-CD45RA Pe/Cy7 (naïve) or anti-CD45RO Brilliant Violet 711 (memory) antibodies using the Cell Sorter SH800S (Sony Biotechnology, Inc., San Jose, CA). Purified $CD4^+$ T cells were activated for indicated time points in 48-well culture plates (Greiner, Monroe, NC) at 2.5 – 3.0 x 10^5 cells/well in media containing 25 U/ml recombinant human IL-2 in an incubator at 37 ^oC and 5 % CO_2. Wells were coated overnight at 4 ^oC with antibodies to CD3, CD28 or CD46 with or without recombinant ICAM-1-Fc (2.0 µg/ml of each in PBS) for general T cell activation. $CD8^+$ T cells were activated in 48-well plates that had been coated overnight at 4 ^oC with antibodies to CD3 (0.5 µg/ml PBS), and CD28 or CD46 with or without recombinant ICAM-1-Fc (2.0 µg/ml of each in PBS) at a concentration of 3.0 x 10^5/well with 25 U/ml rIL-2 ml/media. To test for the effect of E-selectin/CD26E, PECAM-1, VCAM-1, CD99, or iC3b on T cell cytokine production, the cell culture plates were coated with 2 µg/ml of either of these recombinant proteins in conjunction with the activating antibodies. To assess the effects of chemokines on IFN-γ secretion, chemokines were added at indicated concentrations during T cell activation. Cell viability and/or apoptosis was monitored by FACS analysis using a BD LSRFortessa™ flow cytometer (BD Biosciences) or FACSCanto II after Annexin V-APC and Propidium Iodide (both BD Biosciences) staining.

Human Monocyte Purification and *In Vitro* Activation

Human monocytes were isolated from PBMCs (obtained from freshly drawn blood after centrifugation using Lymphoprep separation medium (Corning) to generate a buffy coat) using the MACS human $CD14^+$ Positive Monocyte Isolation Kit (130-050-201, Miltenyi Biotech), according to the manufacturers' instructions. Purity of isolated monocyte populations was typically > 96 %. Monocytes were then cultured in 24-well plates for 6hr to over-night at a concentration of 5.0 x 10^5 cells/well/ml media with or without the addition of 100 ng/ml) LPS. For measurement of impact of LFA-1 activation, monocytes were cultured in 24-wells that had been coated overnight with recombinant ICAM-1-Fc (2.0 µg/ml of each in PBS).

Mouse CD4$^+$ T cell Purification and *In Vitro* Activation

Single cell suspensions of spleen, lymph node, and/or ear cells (see below) were generated and red blood cells lysed using ACK lysis buffer (Life Technologies). CD4$^+$ T cells were isolated by negative selection using the Stem Cell Technologies EasySep^{TM} Mouse CD4$^+$ T Cell Isolation Kit (19752). To obtain pure CD4$^+$ T cell populations, CD4$^+$ cells were sorted using a Sony Biotechnology Cell Sorter SH800S. For *in vitro* T cell activation, 48- or 96-well plates (Greiner CELLSTAR®, Merck, Darmstadt, Germany), were coated with 2 ug/ml anti-mouse CD3 with or without 2 μg/ml ICAM-1-Fc overnight at 4 °C and CD4$^+$ T cells (0.5 – 1.0 x 10^6 per well of 48-well plates or 0.2 x 10^6 per well of 96-well plates) were added to the appropriate wells. One ug/ml of anti-CD28 was added to the media to provide co-stimulation and cells used in indicated assays at desired time points post activation.

Induction of Colitis and Cell Isolation

Splenic CD4$^+$ T cells were isolated from C57BL/6 or *C3*$^{-/-}$ mice using a negative selection CD4 T cell Enrichment Kit (Stemcell Technologies), were stained with anti-CD45RB FITC, anti-CD25APC and anti-CD4 BV421, and sorted on a SH800S cell sorter (Sony Biotechnology) for CD4$^+$ CD25$^-$CD45RB^{hi} (brightest 35%) cells. 2.3 x 10^5 of WT or *C3*$^{-/-}$ cells were injected i.p. into age and sex matched C57BL/10 *Rag2*$^{-/-}$ mice. The mice were sacrificed 7 weeks after adoptive transfer. Spleen and draining lymph node cells were isolated and were stimulated overnight with 1 ug/ml of soluble CD3 (2C11, BioXcell) and CD28 (37.51, BioXcell) antibodies. The following morning, GolgiPlug and GogliStop (BD Biosciences) were added to the cultures for 5 h. The cells were then stained with CD4 and Thy1.2 antibodies and a live/dead fixable near IR (ThermoFisher) and fixed and permeabilized (Cytofix/cytoperm, BD Biosciences) and stained intracellularly with IFN-γ and IL-17A antibodies. All antibodies were from Biolegend unless otherwise indicated.

T Cell Transmigration

Six-well pates (3452, Costar, Corning) with 3 μM pore size inserts were coated with 1 ml of collagen type I (08-115, Millipore Sigma) at 15 μg/ml final concentration in 1 % Acetic acid/water for 1 h at room temperature. Following three washes with sterile 1 x PBS, 1 x 10^5 HUVEC cells (C0035C, ThermoFisher,) resuspended in 1 ml 200 PRF media (M200PRF500,

ThermoFisher) supplemented with 1 x Low Serum Growth Supplement Kit (S003K, ThermoFisher) were plated and grown until about 90 % confluence in 37 ^{o}C and 5 % CO_2. Cells were then treated with 200 ng/ml IL-1β (Biolegend) for 5 h to induce ICAM-1 expression and inserts washed three times with sterile 1 x PBS after which 1 ml Media 200PRF was added to each well. Naive or memory $CD4^+$ T cells were resuspended in 200PRF media at 1 x 10^6 cell/ml and 1.5 x 10^6 T cells added to each insert. Two ml of 200PRF media containing recombinant CXCL10 at 1 μg/ml (Biolegend) was added to each respective bottom well and cells were allowed to transmigrate overnight. Cells retained in the insert (non-migrated cells) and cells from the bottom well (migrated) were collected and analyzed via qPCR and/or FACS analysis for C3 expression and/or cytokine production.

Flow Cytometry

Purified human T cells were left non-activated or harvested at the desired time points post activation, washed in 1 x PBS and then stained for 15 min at room temperature with the LIVE/DEAD® Fixable Dead Cell Stain Kit (Molecular Probes) to monitor viability. Single cell suspensions of mouse cells were treated with TruStain FcX™ (Biolegend) Fc blocking reagent for 15 min at room temperature before life/dead staining. Following two washes with FACS buffer (1 x PBS, pH 7.4, 0.5 % bovine serum albumin (Millipore Sigma, Saint Louis, MO)), cells were stained with fluorochrome-conjugated antibodies to selected surface antigens or with appropriate isotype control antibodies for 30 min on ice. After two washes with FACS buffer samples were fixed and permeabilized using the BD Cytofix/Cytoperm Kit (554714, BD Biosciences) according to the manufacturer's instructions. Cells were then intracellularly stained with the desired fluorochrome-labeled antibodies or a matching isotype control antibody for another 30 mins on ice. In cases were the primary antibody was not directly fluorochrome-conjugated (for example, when human C3/C3b or the C3a/C3adesArg neo-epitope was assessed), cells were washed twice and a second incubation with suitable fluorochrome-labeled secondary antibodies was performed for 30 min on ice. After two final washes, the samples were analyzed on the BD LSRFortessa™ flow cytometer (BD Biosciences) and data analyzed using the FlowJo 10.0.8 software (Ashland, OR).

Cytokine Measurements

Cytokine production by human and mouse T cells and by human monocytes was assessed using the Th1/Th2/Th17 Cytokine Bead Array (BD Biosciences, Oxford, UK) or LEGENDplex Mouse Th cytokine panel (Biolegend), respectively, and analyzed using the BD LSRFortessa^{TM} flow cytometer (BD Biosciences) with FlowJo 10.0.8 software (Ashland, OR). In some instances, IFN-γ production by T cells was assessed using intracellular cytokine staining. IL-1β production by human monocytes was measured using the Human IL-1 beta/IL-1F2 Quantikine ELISA Kit (DLB50, R&D Systems Minneapolis, MN).

PrimeFlow RNA Measurements

The Human PrimeFlow RNA kit (88-18005-210) and C3 type 1 (Alexa Fluor 647) probe set (cat. number PF-210, assay ID VA1-12373-PF) were purchased from Thermo Fisher Scientific. Two million T cells (derived from the different in vitro activation or *ex vivo* activation experiments) were typically stained with antibodies against desired additional intracellular or markers prior to staining with the C3 RNA PrimeFlow Probe Set following the manufacturer's provided protocol. Samples were analyzed either via flow cytometry or confocal microscopy.

OCR and ECAR Measurements

For analysis of the OCR (in pMoles/min) and ECAR (in mpH/min), the Seahorse XF-96 metabolic extracellular flux analyzer was used (Seahorse Bioscience, North Billerica, MA). $CD4^+$ T cells were resuspended in serum-free unbuffered RPMI-1640 medium (R1383; Sigma Aldrich) and were plated onto Seahorse cell plates at 4×10^5 for human T cells and 1.8×10^5 for mouse T cells per well coated with Cell-Tak (CB-40241; Corning, Reinach, Switzerland) to enhance T cell attachment. Perturbation profiling of the use of metabolic pathways by $CD4^+$ T cells was achieved by the addition of oligomycin (O4876; 1 µM), Carbonyl cyanide-*4*-(trifluoromethoxy) phenylhydrazone (FCCP, C2920; 2 µM) and rotenone (R8875; 1 µM - all from Sigma Aldrich, St. Louis, MO). Metabolic parameters were then calculated based on the following formulas:

(1) basal respiration =[OCR(basal-nc)] – [OCR(rotenone)]

(2) ATP coupled respiration = [OCR(basal-nc)] – [OCR(oligomycin)]

(3) maximal respiratory capacity = [OCR(peak-FCCP)] – [OCR(rotenone)

Confocal Microscopy

Fixed and permeabilized cells were stained with the indicated primary antibodies overnight at 4 °C at the manufacturer's suggested dilutions. After two washes, the desired fluorochrome-labeled secondary antibodies were added for 1 h at room temperature. Cells were mounted using Vectashield mounting media containing DAPI (H-1500, Vector Laboratories, Peterborough, UK) and images were obtained in the KCL Nikon Imaging Centre by confocal fluorescence microscopy with the A1R SI Confocal Microscope (360 objective) both from Nikon (Surrey, UK). Experiments were performed at least three times with cells from a different healthy donor each time.

C3/C3a Reconstitution in T Cells from LAD-I Patients

Adenovirus-mediated delivery of C3a mRNA. Non-replicating AdZ-5 adenovirus was used in this study to deliver the human C3a anaphylatoxin into $CD4^+$ T cells. Virus stock was provided as a gift by Dr. Hide Yamamoto (King's College London). Briefly, cDNA coding for the C3a portion of the human *C3* gene was inserted into the pAdZ5-CV5 vector-based non-replicating adenovirus system. Verified purified plasmid (or a control plasmid with scrambled C3a cDNA sequence) was transfected into 293TREx cells to generate adenovirus particles. The adenovirus was used at 10^{-6} PFU/ml concentration and added to the cultures of human $CD4^+$ T cells isolated from patients with LAD-I during in vitro activation with immobilized antibodies to CD3+CD46 with ICAM-1-Fc. Virus-infected cells were assessed by FACS analyses for C3a presence as well as cytokine production at d 5 post transduction/activation.

Electroporation-mediated delivery of C3a mRNA or $C3H_2O$ protein. For electroporation of proteins or mRNAs into $CD4^+$ T cells from LAD-1 deficient patients or healthy donors, 10 µg of PacBlue-labeled $C3H_2O$ or BSA protein or 2 µg of synthesized C3a or eGFP mRNA (Trilink, San Diego, CA) was electroporated into 250,000 bulk $CD4^+$ T cells resuspended in HyClone Electroporation Buffer as per manufacturer's guidelines (MaxCyte ATX Electroporator, Gaithersburg, MD). Purchased serum-purified C3 (Comptech, Tyler, TX), was converted into $C3H_2O$ through five freeze-and-thaw-cycles and $C3H_2O$ and BSA were then labeled utilizing the Pacific Blue™ Protein Labeling Kit (P30012, Thermo Fisher Scientific). After electroporation, cells were rested for 20 min before spin-activation at 300 x *g* for 3 min with plates pre-coated with anti-CD3+CD46 and ICAM-1. Electroporation efficiency was

determined by fluorescence immediately after 3 washes in PBS for protein electroporated samples and mRNA electroporation efficiency was assessed by eGFP fluorescence at 24 h post electroporation, both analyzed by flow cytometry (Attune NXT, Thermo Fisher Scientific). Cells taken for fluorescence analysis were surface-stained with Live-Dead Fixable NEAR-IR stain at a 1:100 dilution in PBS as per manufacturer's guidelines (Thermo Scientific) to exclude dead cells. Where indicated, as control, 2 μg of serum-purified C3a (Comptech) was added to the media of non-electroporated T cells during CD3+CD46+ICAM-1 activation. Samples were assessed for IFN-γ secretion at 12 – 36 hr post activation.

RNA Isolation, cDNA Generation and q-PCR

Total RNA was isolated using the Direct-zol RNA Mini Prep Kit from Zymo Research (Irvine, CA) or the RNAqueous™-Micro Total RNA Isolation Kit (AM1931, Thermo Fisher Scientific) following the manufacturers provided guidelines. Between 50 and 150 ng of total RNA was reverse transcribed into cDNA using the High Capacity Copy DNA (cDNA) Reverse Transcription Kit (4368814) from Applied Biosystems (Foster City, CA) or Protoscript II under the standard protocol directed by the manufacturer with random hexamer priming as included with the enzyme (New England Biolabs, Ipswich, MA). FAM dye-labeled primers used to quantify *C3* mRNA transcription patterns (Hs00163811_m11, 1615290), c-FOS mRNA (Hs00170630_m1, Thermo Scientific) and 18s rRNA (Hs99999901_s1, Thermo Fisher Scientific) or, in some instances the internal VIC dye-labeled 18s control rRNA primers (4318839) from Applied Biosystems. PCR reactions were performed using the Applied Biosystems TaqMan Gene Expression Master Mix (4369016, Thermo Fisher Scientific) according to the manufacturer's protocol at 60 °C annealing temperature. PCR reactions were performed using a C1000 Touch™ Thermo Cycler equipped with the CFX96™ Optical Reaction Module (Bio-Rad, Hercules, CA). Relative quantification (RQ) was performed using the ΔΔCt method (Schmittgen and Livak, 2008) with sample data first normalized to the internal control (18s rRNA) and then to values from appropriate resting or non-treated cell control samples.

Western Blotting

Enriched $CD4^+$ T cells were activated on plates coated with anti-CD3 with or without ICAM1-Fc and incubated for various time points. Snap-frozen cell pellets of 300,000 T cells were resuspended directly in 2 X Laemmli Sample Buffer (Bio-Rad) supplemented with 5 % 2-Mercaptoethanol, denatured at 95 °C for 5 min, and separated using a kD Criterion TGX gel (Bio-Rad). Proteins were then transferred onto nitrocellulose using a Trans-Blot® Turbo™ Midi Nitrocellulose Transfer Pack with the Trans-Blot® Turbo™ Transfer System as per manufacturer's guidelines (Bio-Rad). Membranes were incubated in Odyssey Blocking Buffer with PBS (LI-COR Biosciences, Lincoln, Nebraska, USA) for 1 h at room temperature prior to the addition of primary antibodies. Antibodies against c-FOS (9F6, Cell Signaling Technology) or HSP70 (B-6, sc-7298, Santa Cruz, Dallas, Texas) were diluted 1:1000 and 1:5000, respectively, in blocking buffer and incubated with membranes overnight at 4 °C with rotation. Membranes were then washed 3 x in wash buffer (PBS with 0.1 % Tween-20) and exposed to secondary goat anti-rabbit and goat anti-mouse antibodies (LI-COR Biosciences) at a dilution of 1:5000 in blocking buffer for 1 h at room temperature. After 3 x wash, protein signals were visualized using the Odyssey CLx (LI-COR Biosciences). Relative banding intensity was determined with Image Studio v5.2 (LI-COR Biosciences) and representative graphs generated in Prism 8.

Methicillin-resistant *Staphylococcus aureus* Intradermal Ear Injection

The USA300 clinical isolate (FPR3757) of methicillin-resistant *Staphylococcus aureus* (MRSA) was used in this study. MRSA was plated overnight onto a blood agar plate. A single colony was selected the next morning and grown overnight at 37 °C shaking in 2 ml of tryptic soy broth (112641, Thermo Fisher Scientific) and harvested while in the logarithmic growth phase. Bacteria were washed twice with 1 x PBS. Six- to 9-week-old wild type litter mates or *C3IRES-tdTomato* C57Bl6 mice were injected intradermally using a 29 ½-gauge $^3/_{10}$-ml insulin syringe (BD Biosciences) with MRSA (final OD_{600} = 0.125 in a total volume of 10 µl). Each experiment included 2 to 4 ears per group. At day 7 post infection, the animals were either prepared and used for intravital imaging analysis of immune cells in the ear or culled and immune cells isolated from the ear for ex vivo analysis.

Preparation of Ear Cells

On day 7 post-infection, the ears were excised, washed with 70 % ethanol, and allowed to dry for 5 min. The dorsal and ventral layers were incubated in at 37 °C for 90 min in 1 ml RPMI 1640 medium containing 160 µg/ml of Liberase TL purified enzyme blend (05401160001, Roche Diagnostic Corp.). Following Liberase treatment, the tissue was homogenized for 3 1/2 min in a Medimachine System Homogenizer (Becton Dickinson). The tissue homogenate was then flushed from the Medicon instrument with 10 ml RPMI medium containing 0.05 % DNase (Millipore Sigma) and was filtered using a 50-µm-pore-size cell strainer. For subsequent surface marker staining (e.g. for CD4) and Td tomato signal analysis, the tissue homogenate was pelleted for 10 min at 1,500 rpm and resuspended in FACS buffer.

Intravital Imaging

For imaging experiments, mice were anesthetized with ketamine (85 mg/kg), xylazine (13 mg/kg), and acepromazine (2 mg/kg) in PBS according to the NIH animal protocol and maintained at a core temperature of 37 °C. For two-photon imaging of the MRSA-infected or control ear, the ventral or dorsal side of the ear was gently pressed onto double sided tape that was immobilized on a stainless steel bracket. A pool of saline was placed on the ear and 3D time lapses were captured using a Leica SP8 two-photon microscope equipped with an 12,000-Hz resonant scanner, a 25 × color corrected water-dipping objective (1.0 NA), a quad HyD external detector array, a Mai Tai HP DeepSee Laser (Spectra-Physics) tuned to 905nm and an Insight DS laser (Spectra-Physics) tuned to 1050nm. The following dichroic mirrors were used for most imaging studies: 458nm-LP, 484nm-LP, 562nm-LP or 624LP. For non-GCaMP imaging stacks were acquired at 10-30 sec intervals Z stacks consisted of 7 planes (3 µm step size) and were acquired at 18 sec intervals.

QUANTIFICATION, STATISTICAL ANALYSIS

Analyses were performed using GraphPad PRISM 7 (La Jolla, CA, USA). Data are presented as mean ± SD or median (interquartile range, IQR) for parametric and non-parametric data, respectively, and compared using paired *t*-tests with Bonferroni correction for multiple comparisons, Wilcoxon signed rank tests, the two-tailed Mann-Whitney test, one-way or two-way ANOVA with a Tukey multiple comparison *post hoc* test, as appropriate. p values < 0.05

are denoted statistical significance throughout. All experiments were carried out in triplicate technical and biological replicate unless otherwise stated. FACS plots depicted are representative of a minimum of three replicates (n=3).

Gene set enrichment analysis (GSEA) was performed using GSEA version 3.0 (Subramanian et al., 2005). Gene expression values of circulating and tissue-occupying human $CD4^+$ T cells were obtained from RNA sequencing data deposited in the NCBI Gene Expression Omnibus under accession number GSE94964 (Kumar et al., 2017).
Gene expression values of circulating monocytes and macrophages isolated from tissues were obtained from RNA sequencing data deposited in the NCBI Gene Expression Omnibus under accession number GSE117970 (Cassetta et al., 2019). All monocyte samples were plotted together against all macrophage samples from this dataset. Genesets for testing were sourced from “canonical pathway genes” curated by the MSigDB v7.0 (GSEA). Pathways that were significantly enriched at FDR < 25 % are shown in **Table S1** (Excel file format). Heatmaps were drawn using Morpheus (Broad Institute).

c-FOS ChIP-seq in MCF10A cells was obtained from ENCODE. JASPAR (jaspar.genereg.net) was used to interrogate DNA sequences human *C3* gene promoter for AP-1 binding sites (Khan et al., 2018).

Gene expression values of T cells in the synovia of patients with osteroarthritis, uninflamed rheumatoid arthritis and inflamed rheumatoid arthritis were obtained from bulk RNA sequencing data deposited at Immport under accession code SDY998 (Zhang et al., 2019). Receiver operating characteristics curves were constructed using Prism 8.

DATA AND CODE AVAILABILITY

Deposited datasets analyzed in this study can be found at the Gene Expression Omnibus (GEO) under accession codes GSE94964 (Kumar et al., 2017), GSE117970 (Cassetta et al., 2019) and at Immport under accession code SDY998 (Zhang et al., 2019).

SUPPLEMENTAL INFORMATION

Supplemental Information includes six figures and Supplementary Tables 1 and 2 (both related to Figure 6) in one single PDF file (title: Kolev et al_Supplementary Information), one movie (related to Figure 1) in mp4 format (title: Kolev et al_Supplementary Movie 1_Intravital imaging C3 Td tomato+ cells in MRSA-infected mouse ear d7.mp4) and Supplementary Table 3 (related to Figure 1), in Excel format (title: Kolev et al_Supplementary Table 3_Reactomes in_CD4 T cells_CD8 T cells _myeloid cells.xlsx) can be found with this article online at XXX.

References

Abraham, C., Griffith, J., and Miller, J. (1999). The dependence for leukocyte function-associated antigen-1/ICAM-1 interactions in T cell activation cannot be overcome by expression of high density TCR ligand. J Immunol *162*, 4399-4405.

Alcaide, P., Maganto-Garcia, E., Newton, G., Travers, R., Croce, K.J., Bu, D.X., Luscinskas, F.W., and Lichtman, A.H. (2012). Difference in Th1 and Th17 lymphocyte adhesion to endothelium. J Immunol *188*, 1421-1430.

Alford, S.K., Longmore, G.D., Stenson, W.F., and Kemper, C. (2008). CD46-induced immunomodulatory CD4+ T cells express the adhesion molecule and chemokine receptor pattern of intestinal T cells. J Immunol *181*, 2544-2555.

Arbore, G., and Kemper, C. (2016). A novel "complement-metabolism-inflammasome axis" as a key regulator of immune cell effector function. Eur J Immunol *46*, 1563-1573.

Arbore, G., West, E.E., Rahman, J., Le Friec, G., Niyonzima, N., Pirooznia, M., Tunc, I., Pavlidis, P., Powell, N., Li, Y., *et al.* (2018). Complement receptor CD46 co-stimulates optimal human CD8. Nat Commun *9*, 4186.

Arbore, G., West, E.E., Spolski, R., Robertson, A.A., Klos, A., Rheinheimer, C., Dutow, P., Woodruff, T.M., Yu, Z.X., O'Neill, L.A., *et al.* (2016). T helper 1 immunity requires complement-driven NLRP3 inflammasome activity in CD4+ T cells. Science *352*, aad1210.

Astier, A., Trescol-Biémont, M.C., Azocar, O., Lamouille, B., and Rabourdin-Combe, C. (2000). Cutting edge: CD46, a new costimulatory molecule for T cells, that induces p120CBL and LAT phosphorylation. J Immunol *164*, 6091-6095.

Atarashi, K., Hirata, T., Matsumoto, M., Kanemitsu, N., and Miyasaka, M. (2005). Rolling of Th1 cells via P-selectin glycoprotein ligand-1 stimulates LFA-1-mediated cell binding to ICAM-1. J Immunol *174*, 1424-1432.

Badell, I.R., Russell, M.C., Thompson, P.W., Turner, A.P., Weaver, T.A., Robertson, J.M., Avila, J.G., Cano, J.A., Johnson, B.E., Song, M., *et al.* (2010). LFA-1-specific therapy prolongs allograft survival in rhesus macaques. J Clin Invest *120*, 4520-4531.

Bianchi, E., Denti, S., Granata, A., Bossi, G., Geginat, J., Villa, A., Rogge, L., and Pardi, R. (2000). Integrin LFA-1 interacts with the transcriptional co-activator JAB1 to modulate AP-1 activity. Nature *404*, 617-621.

Buck, M.D., Sowell, R.T., Kaech, S.M., and Pearce, E.L. (2017). Metabolic Instruction of Immunity. Cell *169*, 570-586.

Cardone, J., Le Friec, G., Vantourout, P., Roberts, A., Fuchs, A., Jackson, I., Suddason, T., Lord, G., Atkinson, J.P., Cope, A., *et al.* (2010). Complement regulator CD46 temporally regulates cytokine production by conventional and unconventional T cells. Nat Immunol *11*, 862-871.

Cassetta, L., Fragkogianni, S., Sims, A.H., Swierczak, A., Forrester, L.M., Zhang, H., Soong, D.Y.H., Cotechini, T., Anur, P., Lin, E.Y., *et al.* (2019). Human Tumor-Associated Macrophage and Monocyte Transcriptional Landscapes Reveal Cancer-Specific Reprogramming, Biomarkers, and Therapeutic Targets. Cancer Cell *35*, 588-602.e510.

Chang, C.H., Curtis, J.D., Maggi, L.B., Faubert, B., Villarino, A.V., O'Sullivan, D., Huang, S.C., van der Windt, G.J., Blagih, J., Qiu, J., *et al.* (2013). Posttranscriptional control of T cell effector function by aerobic glycolysis. Cell *153*, 1239-1251.

Chen, M., Wang, C., Li, Z., and Chen, J. (2018). Involvement of JNK signaling pathway in lipopolysaccharide-induced complement C3 transcriptional activation from amphioxus Branchiostoma belcheri. Fish Shellfish Immunol *86*, 196-203.

Chirathaworn, C., Kohlmeier, J.E., Tibbetts, S.A., Rumsey, L.M., Chan, M.A., and Benedict, S.H. (2002). Stimulation through intercellular adhesion molecule-1 provides a second signal for T cell activation. J Immunol *168*, 5530-5537.

Choi, E.Y., Chavakis, E., Czabanka, M.A., Langer, H.F., Fraemohs, L., Economopoulou, M., Kundu, R.K., Orlandi, A., Zheng, Y.Y., Prieto, D.A., *et al.* (2008). Del-1, an endogenous leukocyte-endothelial adhesion inhibitor, limits inflammatory cell recruitment. Science *322*, 1101-1104.

Delgoffe, G.M., Kole, T.P., Zheng, Y., Zarek, P.E., Matthews, K.L., Xiao, B., Worley, P.F., Kozma, S.C., and Powell, J.D. (2009). The mTOR kinase differentially regulates effector and regulatory T cell lineage commitment. Immunity *30*, 832-844.

Doh, J., and Krummel, M.F. (2010). Immunological synapses within context: patterns of cell-cell communication and their application in T-T interactions. Curr Top Microbiol Immunol *340*, 25-50.

Dustin, M.L. (2008). T-cell activation through immunological synapses and kinapses. Immunol Rev *221*, 77-89.

Ellinghaus, U., Cortini, A., Pinder, C.L., Le Friec, G., Kemper, C., and Vyse, T.J. (2017). Dysregulated CD46 shedding interferes with Th1-contraction in systemic lupus erythematosus. Eur J Immunol *47*, 1200-1210.

Elvington, M., Liszewski, M.K., Bertram, P., Kulkarni, H.S., and Atkinson, J.P. (2017). A C3(H20) recycling pathway is a component of the intracellular complement system. J Clin Invest *127*, 970-981.

Feigelson, S.W., Pasvolsky, R., Cemerski, S., Shulman, Z., Grabovsky, V., Ilani, T., Sagiv, A., Lemaitre, F., Laudanna, C., Shaw, A.S., *et al.* (2010). Occupancy of lymphocyte LFA-1 by surface-immobilized ICAM-1 is critical for TCR- but not for chemokine-triggered LFA-1 conversion to an open headpiece high-affinity state. J Immunol *185*, 7394-7404.

Ghannam, A., Fauquert, J.L., Thomas, C., Kemper, C., and Drouet, C. (2014). Human complement C3 deficiency: Th1 induction requires T cell-derived complement C3a and CD46 activation. Mol Immunol *58*, 98-107.

Ghannam, A., Pernollet, M., Fauquert, J.L., Monnier, N., Ponard, D., Villiers, M.B., Péguet-Navarro, J., Tridon, A., Lunardi, J., Gerlier, D., *et al.* (2008). Human C3 deficiency associated with impairments in dendritic cell differentiation, memory B cells, and regulatory T cells. J Immunol *181*, 5158-5166.

Heeger, P.S., and Kemper, C. (2011). Novel roles of complement in T effector cell regulation. Immunobiology.

Hess, C., and Kemper, C. (2016). Complement-Mediated Regulation of Metabolism and Basic Cellular Processes. Immunity *45*, 240-254.

Hogg, N., Patzak, I., and Willenbrock, F. (2011). The insider's guide to leukocyte integrin signalling and function. Nat Rev Immunol *11*, 416-426.

Hosokawa, Y., Hosokawa, I., Ozaki, K., Nakae, H., and Matsuo, T. (2006). Cytokines differentially regulate ICAM-1 and VCAM-1 expression on human gingival fibroblasts. Clin Exp Immunol *144*, 494-502.

Jameson, S.C., and Masopust, D. (2018). Understanding Subset Diversity in T Cell Memory. Immunity *48*, 214-226.

Jiménez-Reinoso, A., Marin, A.V., Subias, M., López-Lera, A., Román-Ortiz, E., Payne, K., Ma, C.S., Arbore, G., Kolev, M., Freeley, S.J., *et al.* (2018). Human plasma C3 is essential for the development of memory B, but not T, lymphocytes. J Allergy Clin Immunol *141*, 1151-1154.e1114.

Kemper, C., and Atkinson, J.P. (2007). T-cell regulation: with complements from innate immunity. Nat Rev Immunol *7*, 9-18.

Khan, A., Fornes, O., Stigliani, A., Gheorghe, M., Castro-Mondragon, J.A., van der Lee, R., Bessy, A., Chèneby, J., Kulkarni, S.R., Tan, G., *et al.* (2018). JASPAR 2018: update of the open-access database of transcription factor binding profiles and its web framework. Nucleic Acids Res *46*, D1284.

King, B.C., Kulak, K., Krus, U., Rosberg, R., Golec, E., Wozniak, K., Gomez, M.F., Zhang, E., O'Connell, D.J., Renström, E., *et al.* (2019). Complement Component C3 Is Highly Expressed in Human Pancreatic Islets and Prevents β Cell Death via ATG16L1 Interaction and Autophagy Regulation. Cell Metab *29*, 202-210.e206.

Kinoshita, S.M., Krutzik, P.O., and Nolan, G.P. (2012). COP9 signalosome component JAB1/CSN5 is necessary for T cell signaling through LFA-1 and HIV-1 replication. PLoS One *7*, e41725.

Kolev, M., Dimeloe, S., Le Friec, G., Navarini, A., Arbore, G., Povoleri, G.A., Fischer, M., Belle, R., Loeliger, J., Develioglu, L., *et al.* (2015). Complement Regulates Nutrient Influx and Metabolic Reprogramming during Th1 Cell Responses. Immunity *42*, 1033-1047.

Kolev, M., Friec, G.L., and Kemper, C. (2014). Complement - tapping into new sites and effector systems. Nat Rev Immunol *14*, 811-820.

Kolev, M., Le Friec, G., and Kemper, C. (2013). The role of complement in CD4+ T cell homeostasis and effector functions. Semin Immunol *25*, 12-19.

Kumar, B.V., Ma, W., Miron, M., Granot, T., Guyer, R.S., Carpenter, D.J., Senda, T., Sun, X., Ho, S.H., Lerner, H., *et al.* (2017). Human Tissue-Resident Memory T Cells Are Defined by Core Transcriptional and Functional Signatures in Lymphoid and Mucosal Sites. Cell Rep *20*, 2921-2934.

Laumonnier, Y., Karsten, C.M., and Köhl, J. (2017). Novel insights into the expression pattern of anaphylatoxin receptors in mice and men. Mol Immunol *89*, 44-58.

Le Friec, G., Sheppard, D., Whiteman, P., Karsten, C.M., Shamoun, S.A., Laing, A., Bugeon, L., Dallman, M.J., Melchionna, T., Chillakuri, C., *et al.* (2012). The CD46-Jagged1 interaction is critical for human TH1 immunity. Nat Immunol *13*, 1213-1221.

Liszewski, M.K., Elvington, M., Kulkarni, H.S., and Atkinson, J.P. (2017). Complement's hidden arsenal: New insights and novel functions inside the cell. Mol Immunol *84*, 2-9.

Liszewski, M.K., Kolev, M., Le Friec, G., Leung, M., Bertram, P.G., Fara, A.F., Subias, M., Pickering, M.C., Drouet, C., Meri, S., *et al.* (2013). Intracellular complement activation sustains T cell homeostasis and mediates effector differentiation. Immunity *39*, 1143-1157.

Lubbers, R., van Essen, M.F., van Kooten, C., and Trouw, L.A. (2017). Production of complement components by cells of the immune system. Clin Exp Immunol *188*, 183-194.

McNamara, H.A., Cai, Y., Wagle, M.V., Sontani, Y., Roots, C.M., Miosge, L.A., O'Connor, J.H., Sutton, H.J., Ganusov, V.V., Heath, W.R., *et al.* (2017). Up-regulation of LFA-1 allows liver-resident memory T cells to patrol and remain in the hepatic sinusoids. Sci Immunol *2*.

Mempel, T.R., Henrickson, S.E., and Von Andrian, U.H. (2004). T-cell priming by dendritic cells in lymph nodes occurs in three distinct phases. Nature *427*, 154-159.

Merle, N.S., Noe, R., Halbwachs-Mecarelli, L., Fremeaux-Bacchi, V., and Roumenina, L.T. (2015). Complement System Part II: Role in Immunity. Front Immunol *6*, 257.

Monks, C.R., Freiberg, B.A., Kupfer, H., Sciaky, N., and Kupfer, A. (1998). Three-dimensional segregation of supramolecular activation clusters in T cells. Nature *395*, 82-86.

Moutsopoulos, N.M., Zerbe, C.S., Wild, T., Dutzan, N., Brenchley, L., DiPasquale, G., Uzel, G., Axelrod, K.C., Lisco, A., Notarangelo, L.D., *et al.* (2017). Interleukin-12 and Interleukin-23 Blockade in Leukocyte Adhesion Deficiency Type 1. N Engl J Med *376*, 1141-1146.

Muller, W.A. (2011). Mechanisms of leukocyte transendothelial migration. Annu Rev Pathol *6*, 323-344.

Novoa, E.A., Kasbekar, S., Thrasher, A.J., Kohn, D.B., Sevilla, J., Nguyen, T., D., S.J., and A., B.J. (2018). Leukocyte adhesion deficiency-I: A comprehensive review of all published cases (The Journal of Allergy and Clinical Immunology: Elsevier), pp. 1418-1420e.1410.

Parameswaran, N., Suresh, R., Bal, V., Rath, S., and George, A. (2005). Lack of ICAM-1 on APCs during T cell priming leads to poor generation of central memory cells. J Immunol *175*, 2201-2211.

Perez, O.D., Mitchell, D., Jager, G.C., South, S., Murriel, C., McBride, J., Herzenberg, L.A., Kinoshita, S., and Nolan, G.P. (2003). Leukocyte functional antigen 1 lowers T cell activation thresholds and signaling through cytohesin-1 and Jun-activating binding protein 1. Nat Immunol *4*, 1083-1092.

Ricklin, D., Hajishengallis, G., Yang, K., and Lambris, J.D. (2010). Complement: a key system for immune surveillance and homeostasis. Nat Immunol *11*, 785-797.

Rudolph, M.G., Stanfield, R.L., and Wilson, I.A. (2006). How TCRs bind MHCs, peptides, and coreceptors. Annu Rev Immunol *24*, 419-466.

Sabatos, C.A., Doh, J., Chakravarti, S., Friedman, R.S., Pandurangi, P.G., Tooley, A.J., and Krummel, M.F. (2008). A synaptic basis for paracrine interleukin-2 signaling during homotypic T cell interaction. Immunity *29*, 238-248.

Schmittgen, T.D., and Livak, K.J. (2008). Analyzing real-time PCR data by the comparative C(T) method. Nat Protoc *3*, 1101-1108.

Subramanian, A., Tamayo, P., Mootha, V.K., Mukherjee, S., Ebert, B.L., Gillette, M.A., Paulovich, A., Pomeroy, S.L., Golub, T.R., Lander, E.S., *et al.* (2005). Gene set enrichment analysis: a knowledge-based approach for interpreting genome-wide expression profiles. Proc Natl Acad Sci U S A *102*, 15545-15550.

Tam, J.C., Bidgood, S.R., McEwan, W.A., and James, L.C. (2014). Intracellular sensing of complement C3 activates cell autonomous immunity. Science *345*, 1256070.

Thatte, J., Dabak, V., Williams, M.B., Braciale, T.J., and Ley, K. (2003). LFA-1 is required for retention of effector CD8 T cells in mouse lungs. Blood *101*, 4916-4922.

Tsujimura, A., Shida, K., Kitamura, M., Nomura, M., Takeda, J., Tanaka, H., Matsumoto, M., Matsumiya, K., Okuyama, A., Nishimune, Y., *et al.* (1998). Molecular cloning of a murine homologue of membrane cofactor protein (CD46): preferential expression in testicular germ cells. Biochem J *330 (Pt 1)*, 163-168.

van der Windt, G.J., and Pearce, E.L. (2012). Metabolic switching and fuel choice during T-cell differentiation and memory development. Immunol Rev *249*, 27-42.

Varga, G., Nippe, N., Balkow, S., Peters, T., Wild, M.K., Seeliger, S., Beissert, S., Krummen, M., Roth, J., Sunderkötter, C., *et al.* (2010). LFA-1 contributes to signal I of T-cell activation and to the production of T(h)1 cytokines. J Invest Dermatol *130*, 1005-1012.

Verma, N.K., Fazil, M.H., Ong, S.T., Chalasani, M.L., Low, J.H., Kottaiswamy, A., P, P., Kizhakeyil, A., Kumar, S., Panda, A.K., *et al.* (2016). LFA-1/ICAM-1 Ligation in Human T Cells Promotes Th1 Polarization through a GSK3β Signaling-Dependent Notch Pathway. J Immunol *197*, 108-118.

Wagner, C., Hänsch, G.M., Stegmaier, S., Denefleh, B., Hug, F., and Schoels, M. (2001). The complement receptor 3, CR3 (CD11b/CD18), on T lymphocytes: activation-dependent up-regulation and regulatory function. Eur J Immunol *31*, 1173-1180.

Walling, B.L., and Kim, M. (2018). LFA-1 in T Cell Migration and Differentiation. Front Immunol *9*, 952.

Wang, G., Liszewski, M.K., Chan, A.C., and Atkinson, J.P. (2000). Membrane cofactor protein (MCP; CD46): isoform-specific tyrosine phosphorylation. J Immunol *164*, 1839-1846.

West, E.E., Kolev, M., and Kemper, C. (2018). Complement and the Regulation of T Cell Responses. Annu Rev Immunol *36*, 309-338.

Wolach, B., Gavrieli, R., Wolach, O., Stauber, T., Abuzaitoun, O., Kuperman, A., Amir, Y., Stepensky, P., Somech, R., and Etzioni, A. (2018). Leukocyte Adhesion Deficiency -A Multicenter National Experience. Eur J Clin Invest, e13047.

Yamamoto, H., Fara, A.F., Dasgupta, P., and Kemper, C. (2013). CD46: the 'multitasker' of complement proteins. Int J Biochem Cell Biol *45*, 2808-2820.

Zhang, F., Wei, K., Slowikowski, K., Fonseka, C.Y., Rao, D.A., Kelly, S., Goodman, S.M., Tabechian, D., Hughes, L.B., Salomon-Escoto, K., *et al.* (2019). Defining inflammatory cell states in rheumatoid arthritis joint synovial tissues by integrating single-cell transcriptomics and mass cytometry. Nat Immunol *20*, 928-942.

Figure 1

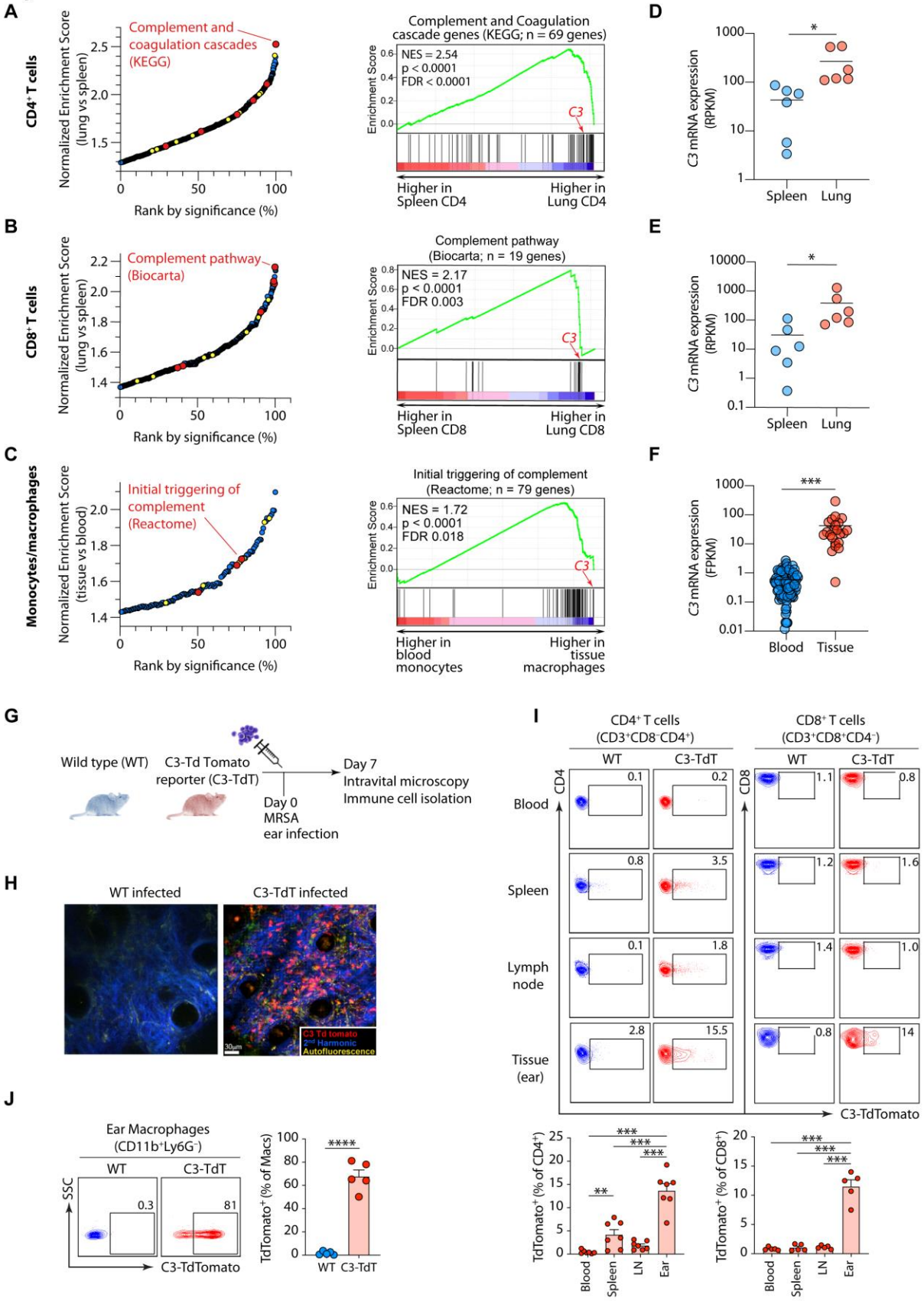
A
CD4+ T cells
Normalized Enrichment Score (lung vs spleen)
Complement and coagulation cascades (KEGG)
Rank by significance (%)
Complement and Coagulation cascade genes (KEGG; n = 69 genes)
NES = 2.54
p < 0.0001
FDR < 0.0001
Enrichment Score
C3
Higher in Spleen CD4
Higher in Lung CD4
D
C3 mRNA expression (RPKM)
Spleen
Lung
B
CD8+ T cells
Normalized Enrichment Score (lung vs spleen)
Complement pathway (Biocarta)
Rank by significance (%)
Complement pathway (Biocarta; n = 19 genes)
NES = 2.17
p < 0.0001
FDR 0.003
Higher in Spleen CD8
Higher in Lung CD8
E
C3 mRNA expression (RPKM)
Spleen
Lung
C
Monocytes/macrophages
Normalized Enrichment Score (tissue vs blood)
Initial triggering of complement (Reactome)
Rank by significance (%)
Initial triggering of complement (Reactome; n = 79 genes)
NES = 1.72
p < 0.0001
FDR 0.018
Higher in blood monocytes
Higher in tissue macrophages
F
C3 mRNA expression (FPKM)
Blood
Tissue
G
Wild type (WT)
C3-Td Tomato reporter (C3-TdT)
Day 0
MRSA ear infection
Day 7
Intravital microscopy
Immune cell isolation
H
WT infected
C3-TdT infected
C3 Td tomato
2nd Harmonic
Autofluorescence
30μm
I
CD4+ T cells (CD3+CD8-CD4+)
CD8+ T cells (CD3+CD8+CD4-)
WT
C3-TdT
CD4
CD8
Blood
Spleen
Lymph node
Tissue (ear)
C3-TdTomato
TdTomato+ (% of CD4+)
TdTomato+ (% of CD8+)
Blood
Spleen
LN
Ear
J
Ear Macrophages (CD11b+Ly6G-)
SSC
C3-TdTomato
TdTomato+ (% of Macs)

Figure 2

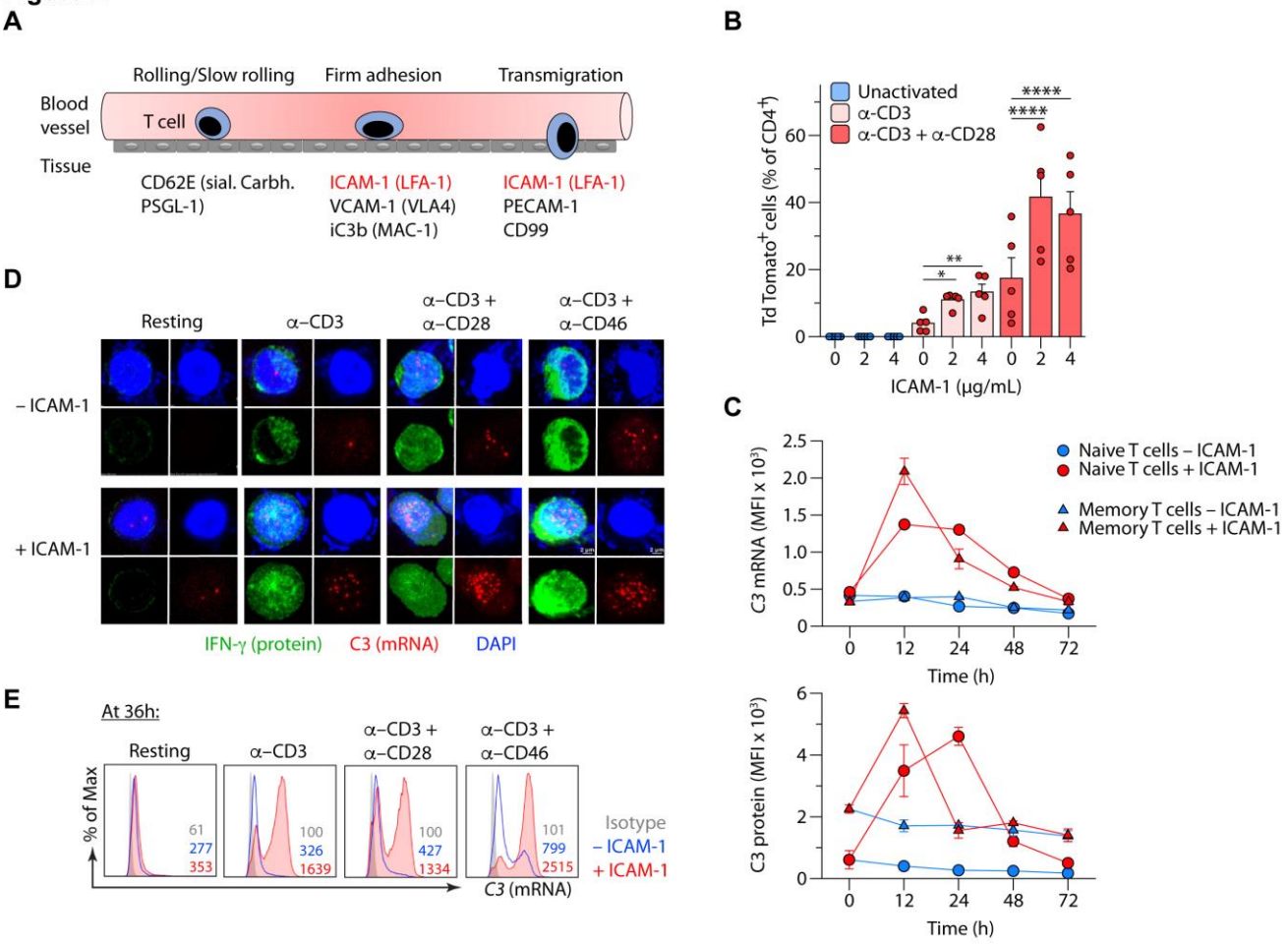
A
Rolling/Slow rolling
Firm adhesion
Transmigration
Blood vessel
T cell
Tissue
CD62E (sial. Carbh.
PSGL-1)
ICAM-1 (LFA-1)
VCAM-1 (VLA4)
iC3b (MAC-1)
ICAM-1 (LFA-1)
PECAM-1
CD99
B
Unactivated
α-CD3
α-CD3 + α-CD28
Td Tomato+ cells (% of CD4+)
ICAM-1 (μg/mL)
C
Naive T cells – ICAM-1
Naive T cells + ICAM-1
Memory T cells – ICAM-1
Memory T cells + ICAM-1
C3 mRNA (MFI x 10³)
C3 protein (MFI x 10³)
Time (h)
D
Resting
α–CD3
α–CD3 + α–CD28
α–CD3 + α–CD46
– ICAM-1
+ ICAM-1
IFN-γ (protein)
C3 (mRNA)
DAPI
E
At 36h:
Resting
α–CD3
α–CD3 + α–CD28
α–CD3 + α–CD46
% of Max
61
277
353
100
326
1639
100
427
1334
101
799
2515
Isotype
– ICAM-1
+ ICAM-1
C3 (mRNA)

Figure 3

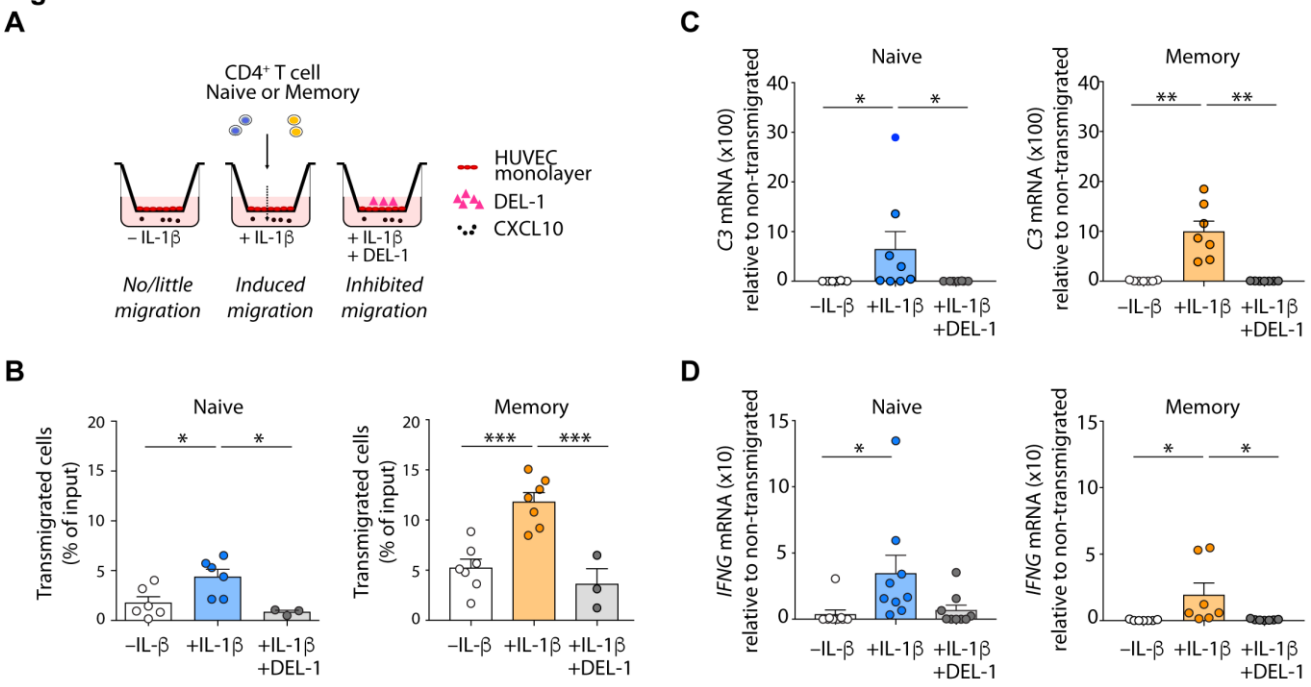
A
CD4+ T cell
Naive or Memory
– IL-1β
+ IL-1β
+ IL-1β
+ DEL-1
HUVEC monolayer
DEL-1
CXCL10
No/little migration
Induced migration
Inhibited migration
B
Naive
Memory
Transmigrated cells (% of input)
–IL-β
+IL-1β
+IL-1β +DEL-1
C
Naive
Memory
C3 mRNA (x100) relative to non-transmigrated
D
Naive
Memory
IFNG mRNA (x10) relative to non-transmigrated

Figure 4

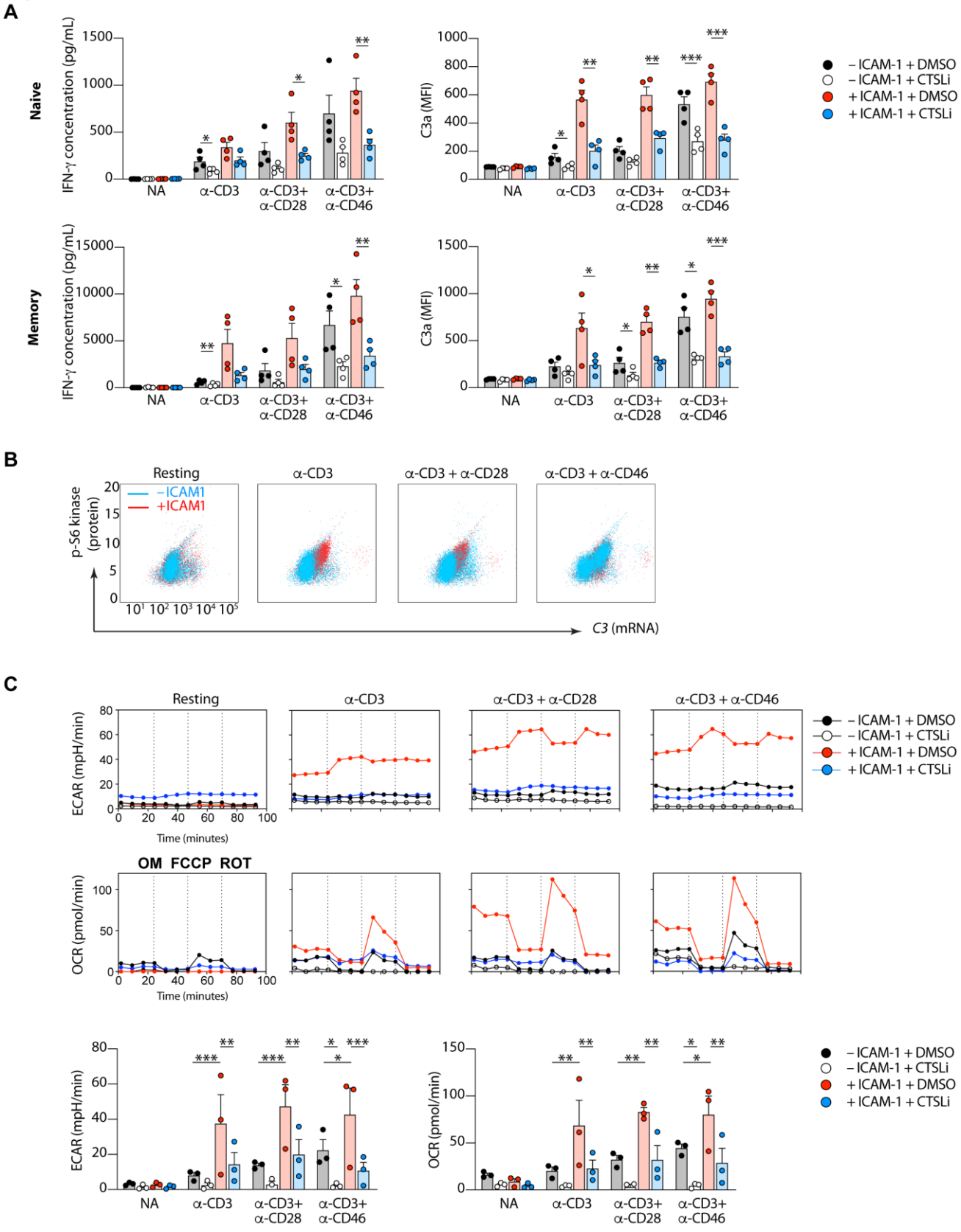
A
Naive
Memory
IFN-γ concentration (pg/mL)
C3a (MFI)
NA
α-CD3
α-CD3+ α-CD28
α-CD3+ α-CD46
– ICAM-1 + DMSO
– ICAM-1 + CTSLi
+ ICAM-1 + DMSO
+ ICAM-1 + CTSLi
B
Resting
α-CD3
α-CD3 + α-CD28
α-CD3 + α-CD46
– ICAM1
+ICAM1
p-S6 kinase (protein)
C3 (mRNA)
C
ECAR (mpH/min)
Time (minutes)
OM FCCP ROT
OCR (pmol/min)

Figure 5

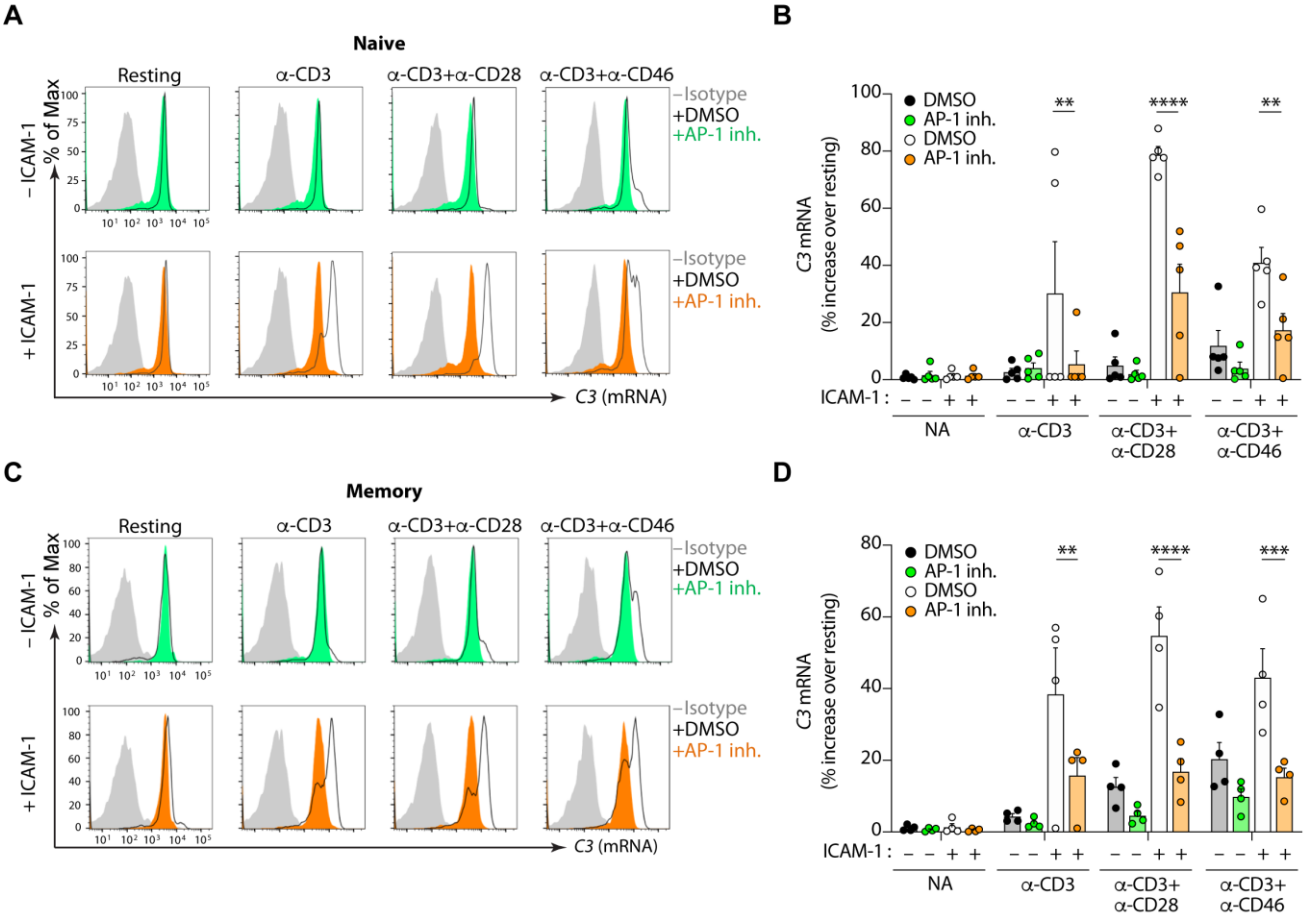
A
Naive
Resting
α-CD3
α-CD3+α-CD28
α-CD3+α-CD46
– ICAM-1
+ ICAM-1
% of Max
Isotype
+DMSO
+AP-1 inh.
C3 (mRNA)
B
C3 mRNA
(% increase over resting)
DMSO
AP-1 inh.
DMSO
AP-1 inh.
**
****
**
ICAM-1 :
NA
α-CD3
α-CD3+
α-CD28
α-CD3+
α-CD46
C
Memory
D
***

Figure 6

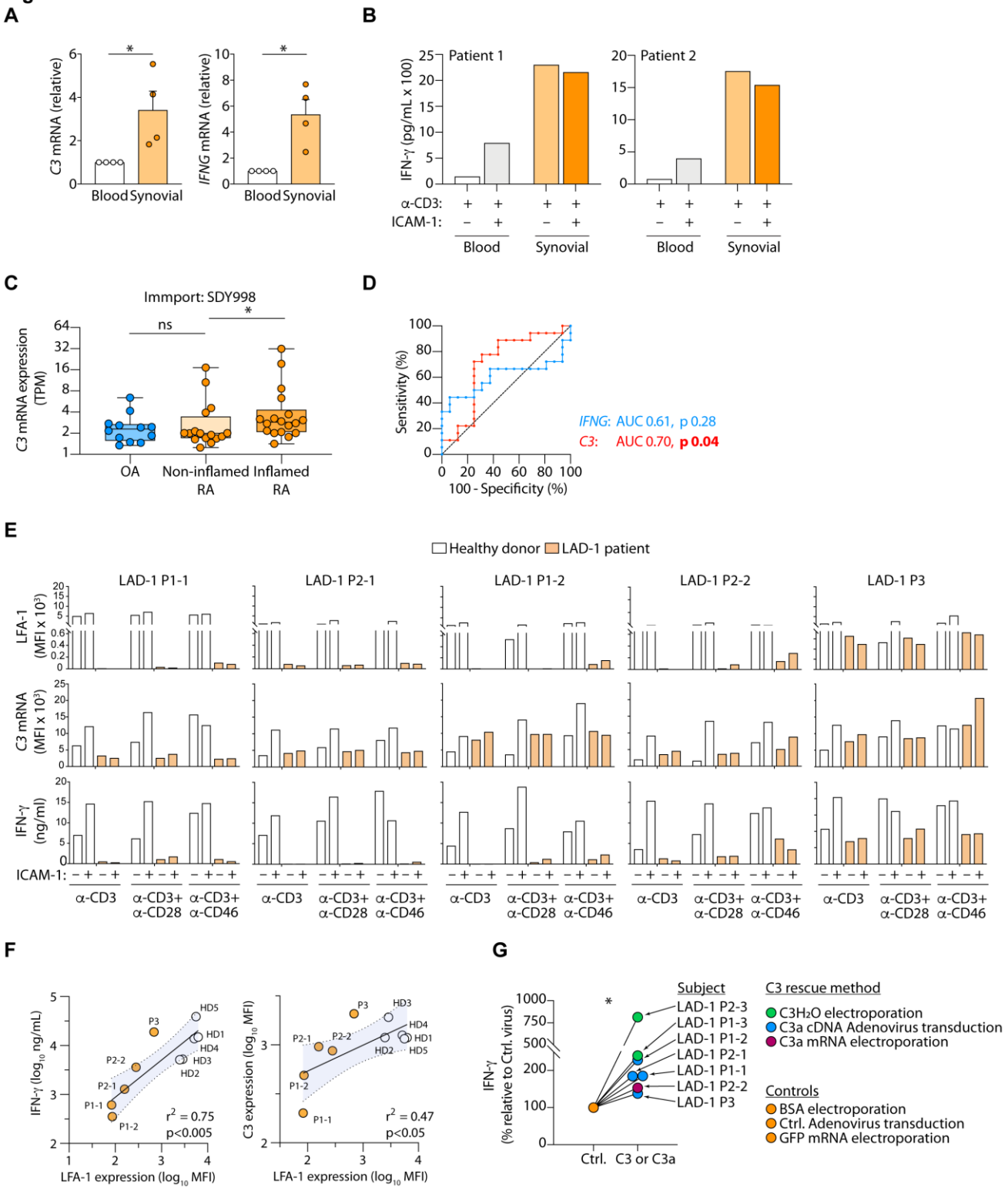
A
C3 mRNA (relative)
IFNG mRNA (relative)
Blood Synovial
B
Patient 1
Patient 2
IFN-γ (pg/mL x 100)
α-CD3:
ICAM-1:
Blood
Synovial
C
Immport: SDY998
ns
*
C3 mRNA expression (TPM)
OA
Non-inflamed RA
Inflamed RA
D
Sensitivity (%)
100 - Specificity (%)
IFNG: AUC 0.61, p 0.28
C3: AUC 0.70, p 0.04
E
Healthy donor
LAD-1 patient
LAD-1 P1-1
LAD-1 P2-1
LAD-1 P1-2
LAD-1 P2-2
LAD-1 P3
LFA-1 (MFI x 10³)
C3 mRNA (MFI x 10³)
IFN-γ (ng/ml)
ICAM-1:
α-CD3
α-CD3+ α-CD28
α-CD3+ α-CD46
F
IFN-γ (log10 ng/mL)
LFA-1 expression (log10 MFI)
r² = 0.75
p<0.005
C3 expression (log10 MFI)
r² = 0.47
p<0.05
HD1
HD2
HD3
HD4
HD5
P1-1
P1-2
P2-1
P2-2
P3
G
IFN-γ (% relative to Ctrl. virus)
Ctrl. C3 or C3a
Subject
LAD-1 P2-3
LAD-1 P1-3
LAD-1 P1-2
LAD-1 P2-1
LAD-1 P1-1
LAD-1 P2-2
LAD-1 P3
C3 rescue method
C3H2O electroporation
C3a cDNA Adenovirus transduction
C3a mRNA electroporation
Controls
BSA electroporation
Ctrl. Adenovirus transduction
GFP mRNA electroporation

SUPPLEMENTARY INFORMATION

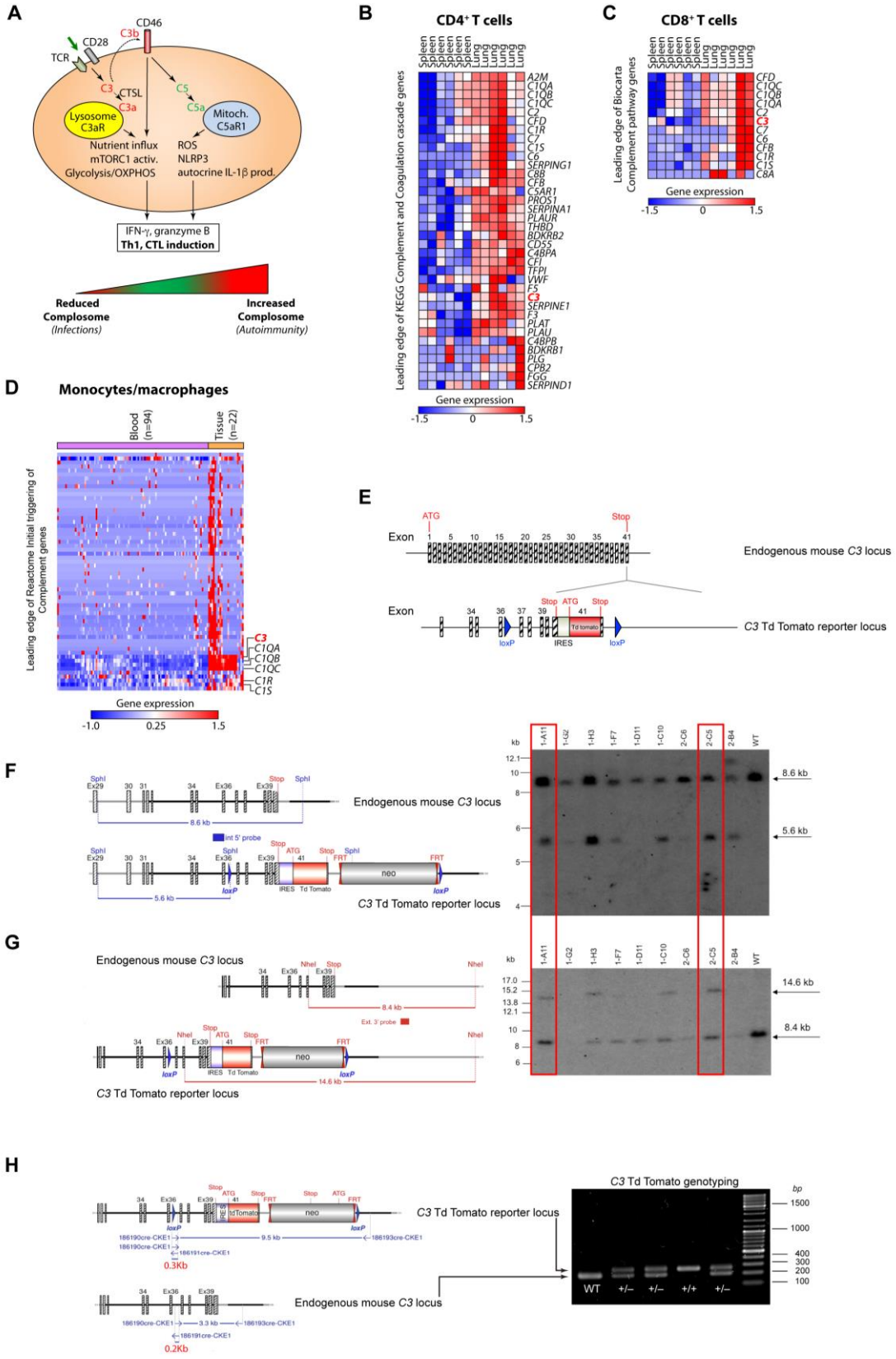

Figure S1. *C3* gene transcription is a feature of immune cells in tissues. Related to Figure 1. (**A**) Model summarizing the mechanistic contributions of autocrine complement C3 signaling to human Th1 induction. TCR stimulation induces processing of intracellular C3 to C3a and C3b by Cathepsin L. C3a engages the C3aR and C3b binds CD46. CD46 ligation by C3b drives processing of intracellular C5 by an unknown protease to C5a, which is bound by C5aR1 intracellularly. C5aR1 drives ROS production and subsequent NLRP3 inflammasome assembly. These events together co-ordinate to mediate the metabolic programming required for pro-inflammatory IFN-γ production and Th1 induction in $CD4^+$ T cells and optimal IFN-γ secretion and granzyme B expression in $CD8^+$ T cells. Low level C3a generation sustaining mTOR-mediated homeostatic cell survival is not depicted. Pathologic dysregulation of this autocrine C3 system contributes to recurrent infections and autoimmunity, respectively. CTL, cytotoxic T cell; CTSL, cathepsin L; mTOR, mammalian target of rapamycin; NLRP3, NLRP3 inflammasome; OXPHOS, oxidative phosphorylation; ROS, reactive oxygen species; TCR, T cell receptor. (**B-D**) Heatmaps of the leading edges (the core enriched genes) of the top ranked complement pathways enriched in $CD4^+$ T cells (**B**), $CD8^+$ T cells (**C**) and macrophages (**D**) from Figures 1A-C. The *C3* gene transcript has been marked in red. (**E**) Schematic depicting the endogenous mouse *C3* locus and the *C3*-Td Tomato reporter locus generated via insertion of an IRES-Td tomato cassette after the endogenous Stop codon and flanked by locus of X-over P1 (*loxP*) sequences. This model permits both *C3* reporter activity as well as generation of conditional knock-out animals. (**F**) Southern blot analyses for the correct 5' homologous recombination in ES cells. Schematic representation of the wild type and recombined alleles with the relevant restriction sites and the position of the probe shown (left panel). The right panel shows the genomic DNA of the tested ES clones in comparison to wild type (WT) DNA. (**G**) Southern blot analyses for the correct 3' homologous recombination in ES cells. Schematic representation of the WT and recombined alleles with the relevant restriction sites and the position of the probe shown (left panel). The right panel shows the genomic DNA of the tested ES clones in comparison to WT DNA. ES clones A11 and C5 (red boxes) were used for injection into C57BL/6 blastocysts and subsequent generation of heterozygous and homozygous *C3*-Td Tomato reporter animals that all showed normal expression levels of endogenous C3 (not shown). (**H**) Representative examples of genotyping WT and *C3*-Td Tomato reporter mice by PCR. The lower band is the wild-type (–) and the upper PCR band the reporter (+) allele.

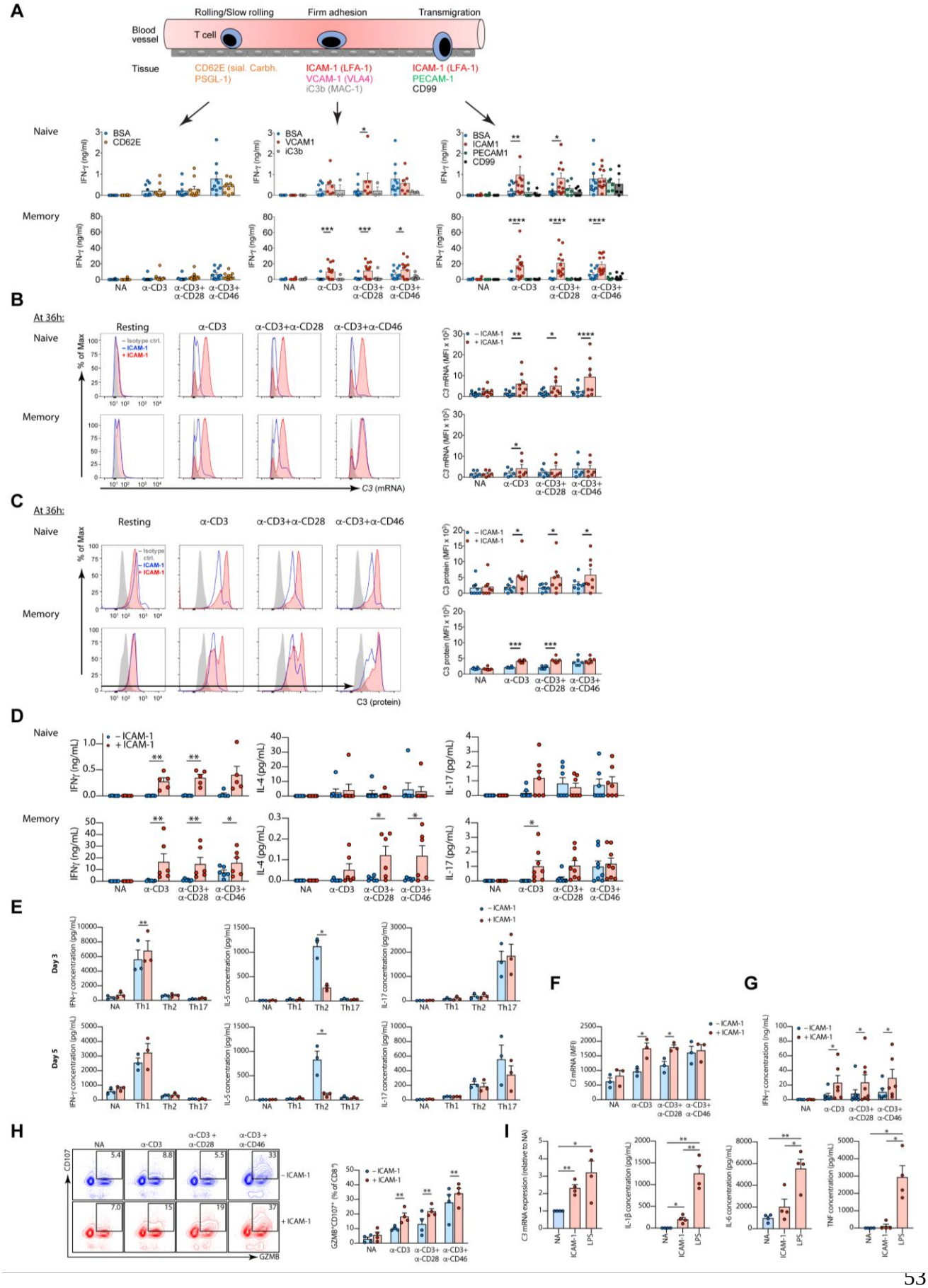
A
Rolling/Slow rolling
Firm adhesion
Transmigration
Blood vessel
T cell
Tissue
CD62E (sial. Carbh. PSGL-1)
ICAM-1 (LFA-1)
VCAM-1 (VLA4)
iC3b (MAC-1)
ICAM-1 (LFA-1)
PECAM-1
CD99
Naive
Memory
BSA
CD62E
VCAM1
iC3b
ICAM1
PECAM1
CD99
IFN-γ (ng/ml)
NA
α-CD3
α-CD3+ α-CD28
α-CD3+ α-CD46
B
At 36h:
Resting
α-CD3
α-CD3+α-CD28
α-CD3+α-CD46
Isotype ctrl.
– ICAM-1
+ ICAM-1
% of Max
C3 (mRNA)
C3 mRNA (MFI x 10³)
C
C3 (protein)
C3 protein (MFI x 10³)
D
IFNγ (ng/mL)
IL-4 (pg/mL)
IL-17 (pg/mL)
E
Day 3
Day 5
IFN-γ concentration (pg/mL)
IL-5 concentration (pg/mL)
IL-17 concentration (pg/mL)
Th1
Th2
Th17
F
C3 mRNA (MFI)
G
IFN-γ concentration (ng/mL)
H
CD107
GZMB
GZMB+CD107+ (% of CD8+)
I
C3 mRNA expression (relative to NA)
IL-1β concentration (pg/mL)
IL-6 concentration (pg/mL)
TNF concentration (pg/mL)
ICAM-1
LPS

Figure S2. ICAM-1 is a key driver of *C3* gene transcription in immune cells. Related to Figure 2. (**A**) ICAM-1 augments IFN-γ production. Purified human naive and memory $CD4^+$ T cells isolated from healthy donors were left non-activated (NA) or activated with immobilized antibodies to CD3, CD3+CD28 or CD3+CD46 with or without plate-bound indicated selectins or integrins for five days and IFN-γ secretion measured (n=6-10). (**B-C**) ICAM-1 increases *C3* gene transcription. Sorted naive and memory T cells were activated with the indicated immobilized antibody combinations with or without ICAM-1 for 60h. *C3* mRNA (**B**) and C3 protein (**C**) levels were then measured by flow cytometry. The left panels each show representative flow cytometry example and right panels show cumulative data from healthy donors (n=6-8). (**D**) IFN-γ, IL-4 and IL-17 secretion by healthy donor naive and memory $CD4^+$ T cells activated or not, as indicated, with plate-bound antibodies in the presence or absence of ICAM-1 (n=5-8). (**E**) IFN-γ, IL-5 and IL-17 secretion by healthy donor naive $CD4^+$ T cells cultured under neutral conditions (NA, non activated) or Th1, Th2 or Th17 skewing conditions in the presence or absence of ICAM-1 (n=3). (**F-H**) Expression of *C3* mRNA (**F**), production of IFN-γ (**G**) and cytotoxic factors (**H**) by healthy donor $CD8^+$ T cells activated, as indicated, in the presence or absence of ICAM-1. Shown in (**H**) are representative flow cytometry plots (left) and cumulative data from n=4-6 independent experiments (right) depicting GMZB and CD107 expression. (**I**) Expression of *C3* mRNA (far left) and production of IL-1β (second from left), IL-6 (second from right) and TNF (far right) in healthy donor monocytes activated, or not, with ICAM-1 or LPS (n=4). Bars show mean + SEM throughout; bars show individual donors and cumulative datsets are from a minimum of n=2-3 independent experiments. *$p < 0.05$, **$p < 0.01$, ***$p < 0.001$, ****$p < 0.0001$.

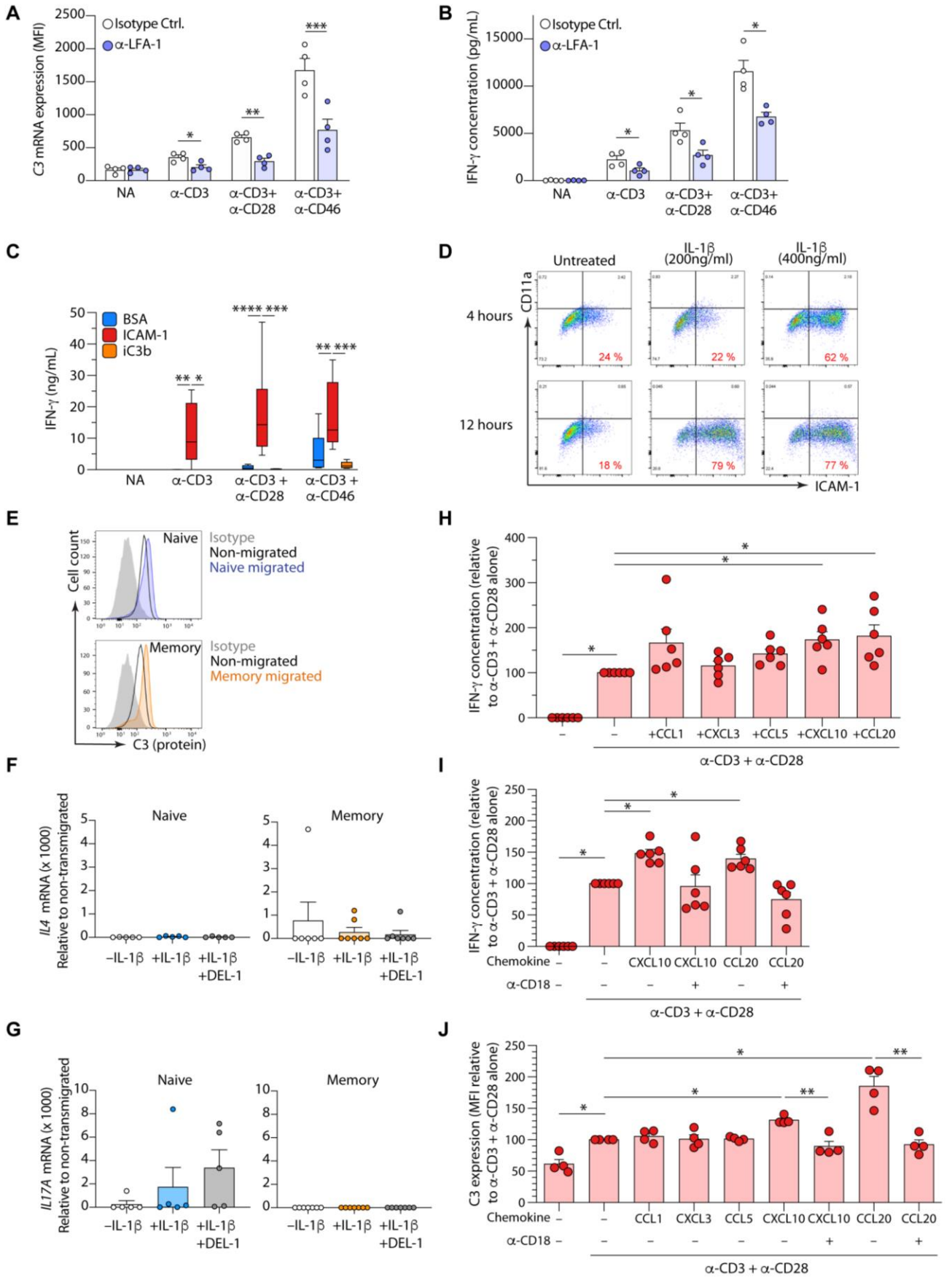
A
C3 mRNA expression (MFI)
Isotype Ctrl.
α-LFA-1
NA
α-CD3
α-CD3+ α-CD28
α-CD3+ α-CD46
B
IFN-γ concentration (pg/mL)
C
IFN-γ (ng/mL)
BSA
ICAM-1
iC3b
D
Untreated
IL-1β (200ng/ml)
IL-1β (400ng/ml)
CD11a
4 hours
12 hours
24 %
22 %
62 %
18 %
79 %
77 %
ICAM-1
E
Cell count
Naive
Isotype
Non-migrated
Naive migrated
Memory
Memory migrated
C3 (protein)
F
IL4 mRNA (x 1000) Relative to non-transmigrated
−IL-1β
+IL-1β
+IL-1β +DEL-1
G
IL17A mRNA (x 1000) Relative to non-transmigrated
H
IFN-γ concentration (relative to α-CD3 + α-CD28 alone)
+CCL1
+CXCL3
+CCL5
+CXCL10
+CCL20
α-CD3 + α-CD28
I
Chemokine
α-CD18
CXCL10
CCL20
J
C3 expression (MFI relative to α-CD3 + α-CD28 alone)
CCL1
CXCL3
CCL5
CXCL10
CCL20

Figure S3. ICAM-1–LFA-1 interaction during diapedesis is required for *C3* gene transcription. Related to Figure 3. (**A-B**) *C3* mRNA expression (**A**) and IFN-γ secretion (**B**) by healthy donor $CD4^+$ T cells 72h post activation as shown in the presence or absence of a blocking antibody to LFA-1, to inhibit homotypic T cell to T cell interactions, or an isotype control antibody (Isotype ctrl.). Shown are cumulative data from n=4 independent experiments normalized to isotype ctrl. (due to donor variation). (**C**) IFN-γ production by healthy donor human $CD4^+$ T cells activated as shown for 72 h in the presence of iC3b (a ligand for the iC3b receptor CD18/CD11b, also known as Mac-1 or CR3) or ICAM-1. Bar and whisker plots show median data from n=4 independent experiments. (**D**) Expression of ICAM-1 and CD11a by HUVECs treated, or not, with increasing concentrations of IL-1β. Shown is one representative example from n=3 independent experiments. (**E**) Representative flow cytometry histograms from n=3 independent experiments showing C3 protein expression in transmigrated and non-transmigrated naive and memory healthy donor $CD4^+$ T cells across a transwell system. (**F-G**) Expression of *IL4* (**F**) and *IL17A* (**G**) mRNA in transmigrated healthy donor naive and memory $CD4^+$ T cells across a transwell system in the presence or absence of IL-1β, with or without DEL-1 (a specific inhibitor of LFA-1–ICAM-1 interaction). Data are from n=5 independent experiments. (**H**) IFN-γ secretion by healthy donor $CD4^+$ T cells cultured in the presence or absence of the indicated chemokines (n=6). (**I**) IFN-γ secretion by healthy donor $CD4^+$ T cells cultured in the presence of CXCL10 or CCL20 with or without a blocking antibody to CD18 (n=4). (**J**) *C3* mRNA expression in healthy donor $CD4^+$ T cells cultured in the presence or absence of the indicated chemokines and antibodies (n=6). Y-axes in (**H-J**) show % relative to anti-CD3+anti-CD28. Bars show mean + SEM. *$p < 0.05$, **$p < 0.01$, ***$p < 0.001$, ****$p<0.0001$.

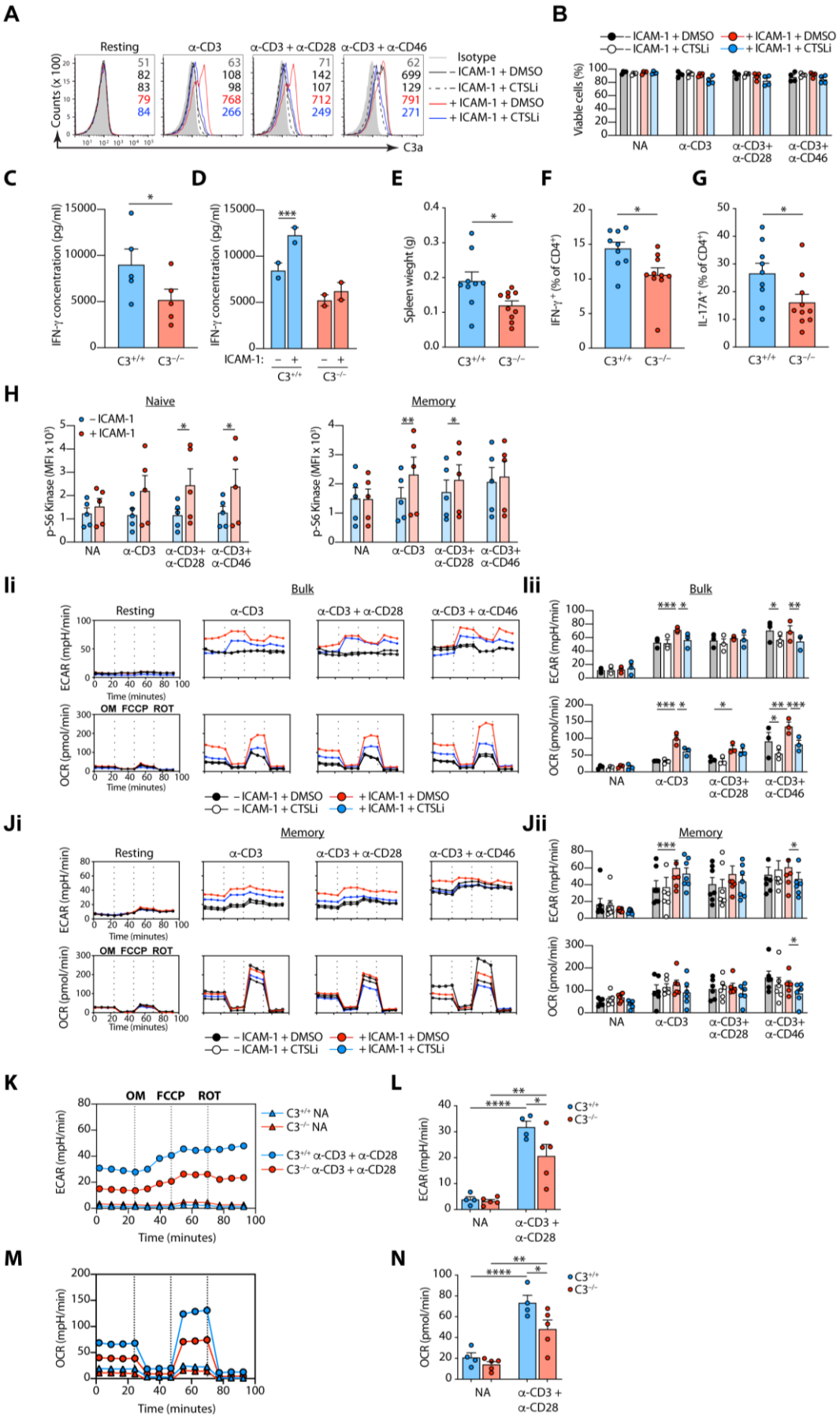
A
Resting
α-CD3
α-CD3 + α-CD28
α-CD3 + α-CD46
Counts (x 100)
C3a
Isotype
– ICAM-1 + DMSO
– ICAM-1 + CTSLi
+ ICAM-1 + DMSO
+ ICAM-1 + CTSLi
B
Viable cells (%)
NA
α-CD3
α-CD3+ α-CD28
α-CD3+ α-CD46
C
IFN-γ concentration (pg/ml)
C3+/+
C3−/−
D
ICAM-1:
E
Spleen wieght (g)
F
IFN-γ+ (% of CD4+)
G
IL-17A+ (% of CD4+)
H
Naive
Memory
p-S6 Kinase (MFI x 10³)
– ICAM-1
+ ICAM-1
Ii
Bulk
ECAR (mpH/min)
OCR (pmol/min)
OM FCCP ROT
Time (minutes)
Iii
Ji
Jii
K
L
M
N

Figure S4. ICAM-1 drives C3-dependent metabolic reprogramming during T cell activation. Related to Figure 4. (**A**) Representative flow cytometry histogram from n=4 independent experiments showing intracellular C3a in healthy donor $CD4^+$ T cells activated as shown in the presence or absence of ICAM-1 with, or without, a cell-permeable cathepsin L inhibitor (CTSLi) at 72h post activation. Cumulative data is shown in **Figure 4A**. (**B**) Viability of $CD4^+$ T cells after 72h of activation the presence or absence of ICAM-1 with or without a CTSL inhibitor (n=4 independent experiments). (**C**) IFN-γ production by *C3* wild-type ($C3^{+/+}$) and *C3* knockout ($C3^{-/-}$) $CD4^+$ mouse T cells activated *in vitro* with anti-CD3 + anti-CD28. (**D**) IFN-γ production by $C3^{+/+}$ and $C3^{-/-}$ $CD4^+$ mouse T cells activated *in vitro* with anti-CD3 + anti-CD28 in the presence or absence of ICAM-1. Data in **C-D** are from n-2 independent expereiments. (**E-G**) Transfer colitis with $C3^{+/+}$ (n=9) and $C3^{-/-}$ (n=10) mouse $CD4^+CD25^-CD45RB^{hi}$ cells into $Rag2^{-/-}$.Bl10 recipients. Shown are splenic weights (**E**), percentage of IFN-γ positive (**F**) and IL-17 positive (**G**) recovered cells 7 weeks later. (**H**) Phosphorylated S6 kinase (p-S6) in healthy donor naive and memory $CD4^+$ T cells activated as shown in the presence or absence of ICAM-1. Shown are cumulative data from n=4 independent experiments. (**I-J**) ECAR (glycolysis) and OCR (OXPHOS) measurements at 36 h in healthy donor bulk (**I**) and memory (**J**) $CD4^+$ T cells activated as shown in the presence or absence of ICAM-1 with, or without, a CTSL inhibitor. Shown are representative examples of the Seahorse analysis profiles (**Ii** and **Ji**) and cumulative data of the maximal respiration and glycolysis from n=3-6 independent experiments (**Iii** and **Jii**). (**K-N**) ECAR (glycolysis) (**K-L**) and OCR (OXPHOS) (**M-N**) measurements in $CD4^+$ T cells from $C3^{+/+}$ and $C3^{-/-}$ mice, activated, or not, with anti-CD3 + anti-CD28 antibodies. Shown are representative (**K** and **M**) examples and cumulative data (**L** and **N**) from n=3 independent experiments. NA, non-activated; FCCP, p-trifluoromethoxyphenyl hydrazine; OM, oligomycin; ROT, rotenone. Bars show mean ± SEM throughout. *$p < 0.05$, **$p < 0.01$, ***$p < 0.005$, ****p<0.001.

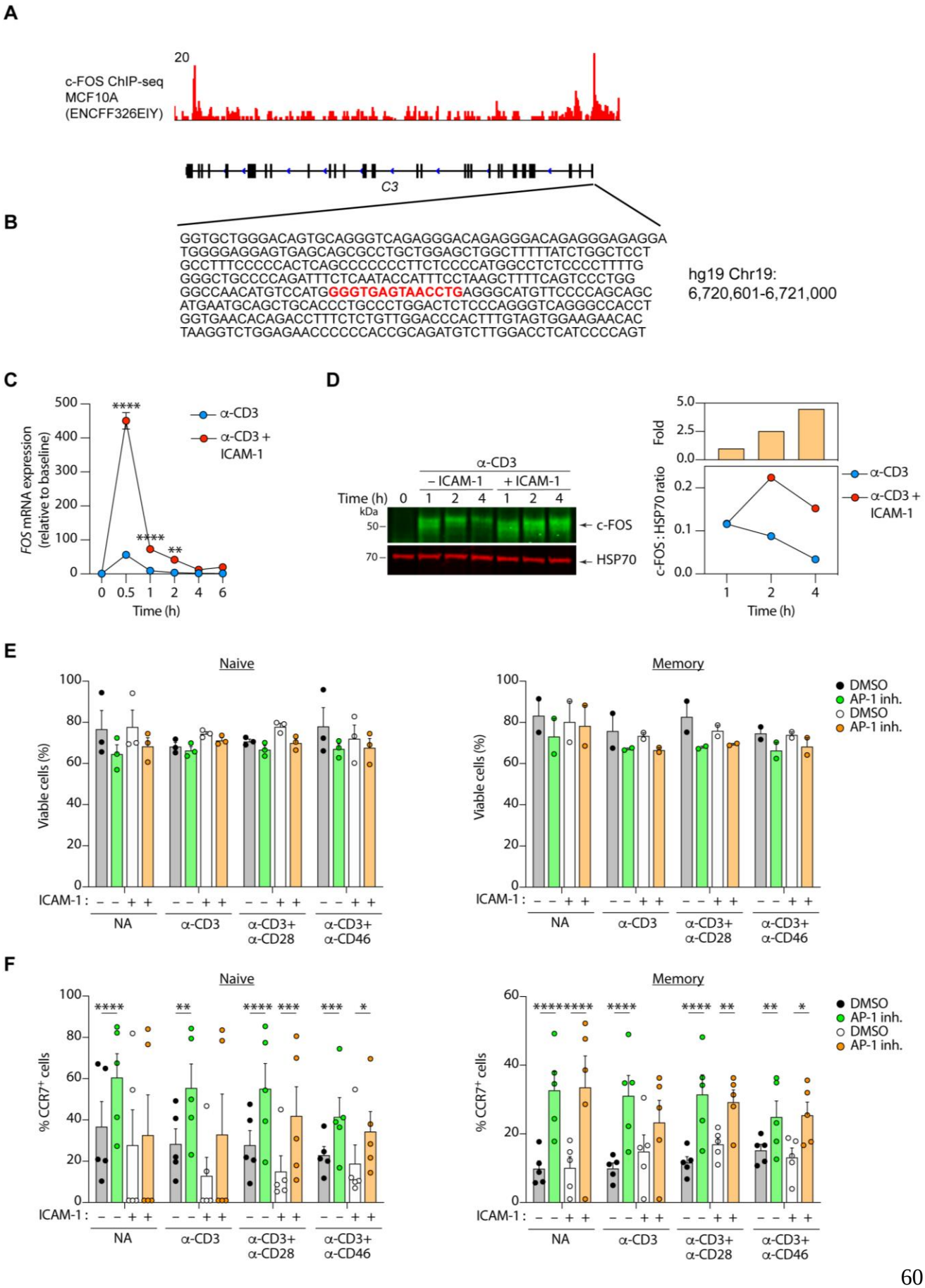
A
20
c-FOS ChIP-seq
MCF10A
(ENCFF326EIY)
C3
B
GGTGCTGGGACAGTGCAGGGTCAGAGGGACAGAGGGACAGAGGGAGAGGA
TGGGGAGGAGTGAGCAGCGCCTGCTGGAGCTGGCTTTTTATCTGGCTCCT
GCCTTTCCCCCACTCAGCCCCCCCTTCTCCCCATGGCCTCTCCCCTTTTG
GGGCTGCCCCAGATTTCTCAATACCATTTCCTAAGCTTTTCAGTCCCTGG
GGCCAACATGTCCATGGGGTGAGTAACCTGAGGGCATGTTCCCCAGCAGC
ATGAATGCAGCTGCACCCTGCCCTGGACTCTCCCAGGGTCAGGGCCACCT
GGTGAACACAGACCTTTCTCTGTTGGACCCACTTTGTAGTGGAAGAACAC
TAAGGTCTGGAGAACCCCCCACCGCAGATGTCTTGGACCTCATCCCCAGT
hg19 Chr19:
6,720,601-6,721,000
C
FOS mRNA expression (relative to baseline)
α-CD3
α-CD3 + ICAM-1
Time (h)
D
α-CD3
– ICAM-1
+ ICAM-1
Time (h)
kDa
c-FOS
HSP70
Fold
c-FOS : HSP70 ratio
E
Naive
Memory
Viable cells (%)
DMSO
AP-1 inh.
ICAM-1 :
NA
α-CD3
α-CD3+ α-CD28
α-CD3+ α-CD46
F
% CCR7+ cells

Figure S5. LFA-1 induces *C3* gene expression in CD4$^+$ T cells via AP-1. Related to Figure 5. (**A-B**) c-FOS ChIP-seq screenshot at the human *C3* gene locus (**A**) and C3 promoter sequence with AP-1 binding DNA motif highlighted in red (**B**). Data source for ChIP-seq is indicated and motif analysis is from JASPAR. (**C-D**) *FOS* mRNA (**C**) and protein (**D**) expression in naive human CD4$^+$ T cells activated with anti-CD3 with or without ICAM-1 for the indicated time points. (**C-D**) are representatives from n=2 (**C**) and n=3 (**D**) experiments carried out. The Western blot in (**D**) has been quantified on the right and the fold c-FOS protein induction by ICAM-1 is shown. (**E-F**) Viability of (**E**) and CCR7 expression on (**F**) naive (left) and memory (right) CD4$^+$ T cells activated as indicated in the presence or absence of ICAM-1 with or without a cell-permeable AP-1 inhibitor (AP-1 inh.) or DMSO carrier control at 72 h post activation. Shown are cumulative data from 2-5 independent experiments (**E** and **F**)**.** NA, not-activated. Error bars represent mean ± SEM, dots show individual donors. *$p < 0.05$, **$p < 0.01$, ***$p < 0.001$, ****$p<0.0001$.

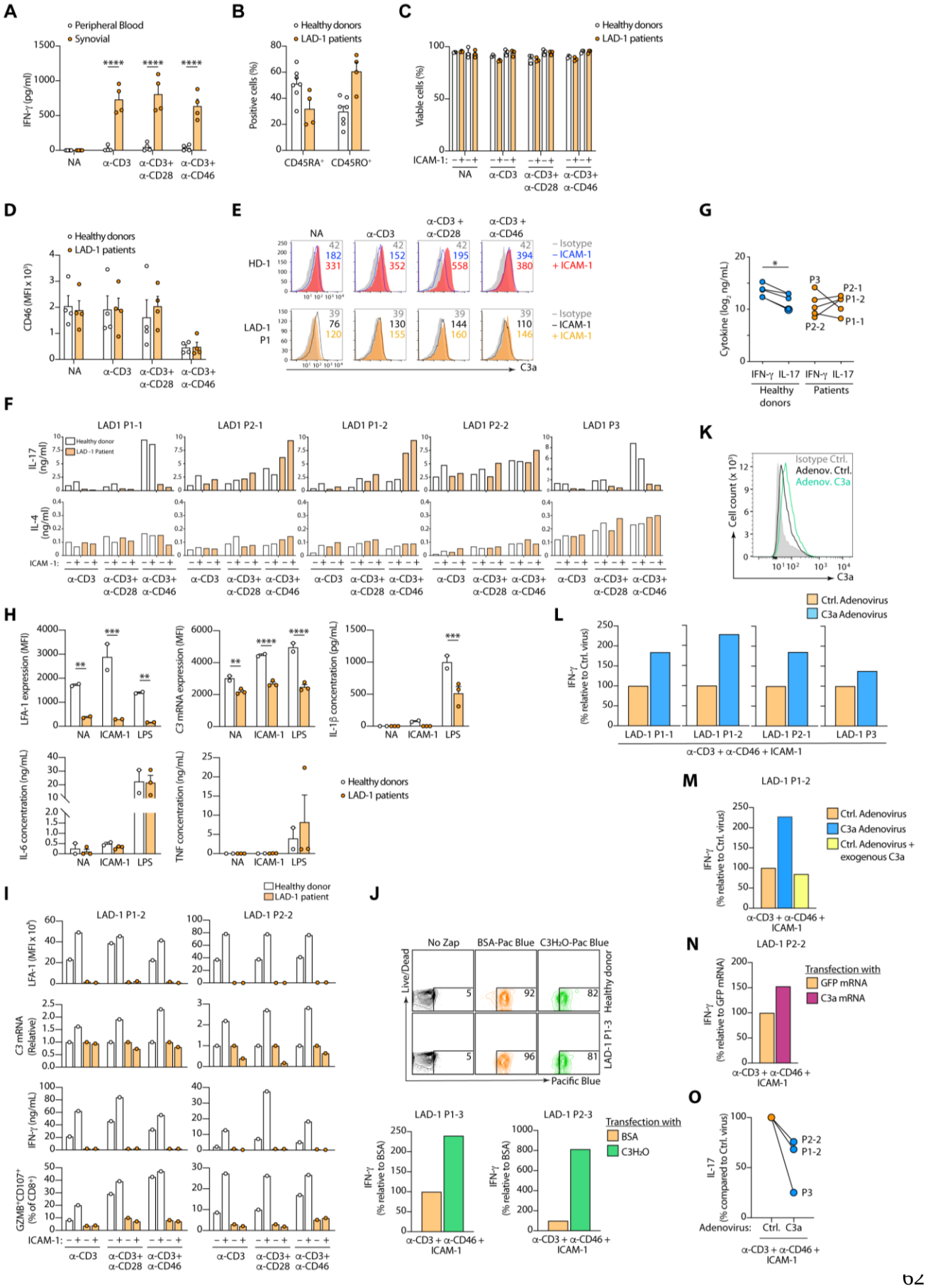
A
Peripheral Blood
Synovial
IFN-γ (pg/ml)
NA
α-CD3
α-CD3+ α-CD28
α-CD3+ α-CD46
B
Healthy donors
LAD-1 patients
Positive cells (%)
CD45RA+
CD45RO+
C
Healthy donors
LAD-1 patients
Viable cells (%)
ICAM-1:
D
Healthy donors
LAD-1 patients
CD46 (MFI x 10³)
E
HD-1
LAD-1 P1
Isotype
– ICAM-1
+ ICAM-1
C3a
F
LAD1 P1-1
LAD1 P2-1
LAD1 P1-2
LAD1 P2-2
LAD1 P3
Healthy donor
LAD-1 Patient
IL-17 (ng/ml)
IL-4 (ng/ml)
ICAM -1:
G
Cytokine (log2 ng/mL)
P3
P2-1
P1-2
P2-2
P1-1
IFN-γ
IL-17
Healthy donors
Patients
K
Isotype Ctrl.
Adenov. Ctrl.
Adenov. C3a
Cell count (x 10³)
C3a
H
LFA-1 expression (MFI)
C3 mRNA expression (MFI)
IL-1β concentration (pg/mL)
IL-6 concentration (ng/mL)
TNF concentration (ng/mL)
NA
ICAM-1
LPS
Healthy donors
LAD-1 patients
L
Ctrl. Adenovirus
C3a Adenovirus
IFN-γ (% relative to Ctrl. virus)
LAD-1 P1-1
LAD-1 P1-2
LAD-1 P2-1
LAD-1 P3
α-CD3 + α-CD46 + ICAM-1
M
LAD-1 P1-2
Ctrl. Adenovirus
C3a Adenovirus
Ctrl. Adenovirus + exogenous C3a
IFN-γ (% relative to Ctrl. virus)
α-CD3 + α-CD46 + ICAM-1
I
Healthy donor
LAD-1 patient
LAD-1 P1-2
LAD-1 P2-2
LFA-1 (MFI x 10³)
C3 mRNA (Relative)
IFN-γ (ng/mL)
GZMB+CD107+ (% of CD8+)
ICAM-1:
J
No Zap
BSA-Pac Blue
C3H2O-Pac Blue
Live/Dead
Pacific Blue
Healthy donor
LAD-1 P1-3
LAD-1 P1-3
LAD-1 P2-3
Transfection with
BSA
C3H2O
IFN-γ (% relative to BSA)
α-CD3 + α-CD46 + ICAM-1
N
LAD-1 P2-2
Transfection with
GFP mRNA
C3a mRNA
IFN-γ (% relative to GFP mRNA)
α-CD3 + α-CD46 + ICAM-1
O
IL-17 (% compared to Ctrl. virus)
P2-2
P1-2
P3
Adenovirus:
Ctrl.
C3a
α-CD3 + α-CD46 + ICAM-1

Figure S6. LAD-1 disease causes failure of *C3* expression and normal immune cell function. Related to Figure 6. (**A**) IFN-γ production by paired $CD4^+$ T cells from blood (white bars) and synovial fluid (orange bars) of pediatric patients with juvenile idiopathic oligo-arthritis (n=4; Table S2). See also **Figure 6A**. Bars show mean+SEM. (**B**) Blood-circulating naive ($CD45RA^+CD45RO^-$) and memory ($CD45RA^-CD45RO^+$) $CD4^+$ T cells of patients with LAD-1 compared to age- and sex-matched healthy controls. Shown are mean+SEM from three patients, one of whom donated twice, and five controls. Comparisons between patients and controls are not significant. (**C**) Viability of $CD4^+$ T cells of patients with LAD-1 disease compared to age- and sex-matched healthy controls activated as shown with and without ICAM-1 for 72 h (n=3). Shown are mean+SEM from three patients, two of whom donated twice, and five controls. (**D**) CD46 expression (and activation-induced down-regulation) on $CD4^+$ T cells of patients with LAD-1 (Table S3) compared to healthy controls activated as shown for 12 h. Shown are mean+SEM from three patients, one of whom donated twice, and five controls. (**E**) C3a generation in $CD4^+$ T cells of patients with LAD-1 compared to healthy controls activated, as shown, in the presence or absence of ICAM-1 for 72h. Shown are representative flow cytometry histograms from one patient and one healthy control. (**F**) IL-17 and IL-4 secretion by peripheral blood $CD4^+$ T cells from patients with LAD-1 disease and age- and sex-matched controls activated *in vitro* as shown with, or without, ICAM-1 for 72 h. Data are from three patients, two of whom donated twice, and five controls. Bars represent mean of duplicate measurements per subject. (**G**) Proportion of Th1 vs. Th17 cells in healthy donors and patients with LAD-1 disease 72 h post CD3+CD46 activation. (**H**) LFA-1 expression (top left), *C3* mRNA (top middle), IL-1β (top right), IL-6 (bottom left) and TNF (bottom right) secretion by peripheral blood monocytes from patients with LFA-1 mutations (LAD-1 disease) and age- and sex-matched controls stimulated, or not, with ICAM-1 or LPS, as shown, for 72 h. Data are from two patients (P1, who donated twice, and P2) and two matched controls. (**I**) LFA-1 expression (top), *C3* mRNA (second from top), IFN-γ secretion (second from bottom) and production of Granzyme B and CD107 by peripheral blood $CD8^+$ T cells from patients with LFA-1 mutations (LAD-1 disease) (see Table S3) and age- and sex-matched controls activated *in vitro*, as shown, with, or without ICAM-1 for 72 h. Data are from two patients (P1 and P2) and two matched controls. (**J**) IFN-γ secretion by peripheral blood $CD4^+$ T cells from two patients with LAD-1 disease after electroporation with BSA or intact $C3H_2O$ protein. Cells were activated with anti-CD3+CD46+ICAM-1 after transduction for 72 h. Shown above are representative flow cytometry plots of the efficiency of protein electroporation using pacific blue-labelled BSA or $C3H_2O$. (**K-L**) Representative flow cytometry histogram of C3a in peripheral blood $CD4^+$ T cells from patients with LAD-1 disease transduced with adenovirus encoding C3a or control virus (**K**) and IFN-γ secretion (**L**) by peripheral blood $CD4^+$ T cells from three patients with LAD-1 disease, two of whom donated twice, after transduction with control adenovirus or adenovirus encoding C3a. Cells were activated with anti-CD3+CD46+ICAM-1 after transduction for 72 h. (**M**) IFN-γ secretion by peripheral blood $CD4^+$ T cells from LAD-1 patient P1 after transduction with control adenovirus or adenovirus encoding C3a. Cells were activated with anti-CD3+CD46+ICAM-1 after transduction for 72 h and exogenous C3a was also provided to cells transduced with control adenovirus. (**N**) IFN-γ secretion by peripheral blood $CD4^+$ T cells from LAD-1 patient P2 after electroporation with mRNA encoding GFP or C3a. Cells were activated with anti-CD3+CD46+ICAM-1 after telectroporation for 72 h. (**O**) IL-17 secretion by peripheral blood $CD4^+$ T cells from three patients with LAD-1 disease after transduction with control adenovirus

or adenovirus encoding C3a. Cells were activated with anti-CD3+CD46+ICAM-1 after transduction for 72h. NA, non-activated; *$p < 0.05$, **p<0.01, ***p<0.001, ****p<0.0001.

Patient	*Age (years)*	*Sex*	*Treatment*	*Active joint count*	*ESR (median IQR)*
1	7.9	F	Naive	1	28H mm/hr
2	8.2	M	Ibuprofen - 400 mg PO Cetirizine - 10 mg	1	17H mm/hr
3	4.4	F	Methotraxate 10 mg once a week Folic acid 1 mg od	3	60H mm/hr
4	7.3	F	Methotraxate 10 mg once a week Maxidex eye drops, one drop in each eye	1	4H mm/hr

Table S2. Characteristics of the four JIA patients included in this study. Related to Figure 6. *ESR, erythrocyte sedimentation rate; IQR, interquartile range*

Table S3. Characteristics of LAD-1 patients (1-3, high to low disease severity). Related to Figure 6. *, LAD-1 Patient 3 was published (Moutsopoulos et al., NEJM, 2017).

Patient	Sex	Race/ Ethnicity	Age at diagn.	Mutation	Somatic reversion	Skin lesions	Warts	Perido. disease	HSCT	Current status
1	F	Hispanic	0.5	Homozyg. c.1412 del 2114 del exons 12 and 13	No	No	Yes	Yes	No	Alive 23
2	M	Hispanic	2	Homozyg.c.1412del 2114 del exon 12 and 13	No	Yes	Yes	Yes	Yes – failure to engraft	Alive 22
3*	M	White	4	Homozyg.c.IVS15−2A→G p.D750_K755	Yes	Yes	No	Yes	No	Alive 23